Apéndice C

PUBLICACIONES

Durante la realización de este trabajo de investigación se han presentado los resultados en diversas publicaciones, que se adjuntan en este apéndice:

Autores: *A. Pérez, A.M. Sánchez, J.R. Regué, M. Ribó, J.P. Rodríguez-Cepeda, F.J. Pajares*
Título: *Characterization of power-line filters and electronic equipment for conducted-emission prediction*
Revista: *IEEE Transactions on Electromagnetic Compatibility*
Publicación: *Aceptado, pendiente de publicación*

Autores: *A.M. Sánchez, A. Pérez, J.R. Regué, M. Ribó, P. Rodríguez-Cepeda, F.J. Pajares*
Título: *Optimization of the Scattering Parameter Measurement of Electronic Equipment with Conducted Emissions*
Tipo de participación: *Poster*
Congreso: *EMC Europe Workshop 2007*
Publicación: *CD de artículos*
Lugar de celebración: *París - Francia*
Fecha: *Junio 2007*

Autores: *A. Pérez, J.R. Regué, M. Ribó, A.M. Sánchez, F.J. Pajares, D. Badia*
Título: *Circuital Characterization of an Electronic Equipment for Narrow-Band Conducted Emissions*
Tipo de participación: *Ponencia*
Congreso: *International Symposium on Electromagnetic Compatibility EMC Europe 2006*
Publicación: *Symposium Record*, pp. 1035-1040
Lugar de celebración: *Barcelona - España*
Fecha: *Septiembre 2006*

Autores: *R. Regué, M. Ribó, D. Duran, D. Badia, A. Pérez*
Título: *Common and Differential Mode Characterization of EMI Power-Line Filters from S-parameters Measurements*
Tipo de participación: *Ponencia*
Congreso: *IEEE International Symposium on Electromagnetic Compatibility*
Publicación: *Symposium Record*, pp. 610-615
Lugar de celebración: *Santa Clara - USA*
Fecha: *Agosto 2004*

Autores: *J.R. Regué, M. Ribó, D. Duran, D. Badia, A. Pérez*
Título: *Measurement and modeling of noise source impedance of electronic equipment*
Tipo de participación: Ponencia
Congreso: *International Symposium on Electromagnetic Compatibility EMC Europe 2004*
Publicació: *Symposium Record*, pp. 150-154
Lugar de celebración: *Eindhoven - Holanda*
Fecha: *Septiembre 2004*

Autores: *A. Pérez, A.M. Sánchez, G. Roig, J.R. Regué, M. Ribó, P. Rodríguez-Cepeda, F.J. Pajares*
Título: *Método de medida mejorado de la impedancia de entrada de equipos electrónicos*
Tipo de participación: *Ponencia*
Congreso: *Congreso Nacional de la Unión Científica Internacional de Radio (URSI)*
Publicación: *CD de artículos*
Lugar de celebració: *Tenerife - España*
Fecha: *Septiembre 2007*

Autores: *A. Pérez, J.R. Regué, M. Ribó, A.M. Sánchez, F.J. Pajares, D. Badia*
Título: *Caracterización Circuital de un Equipo Electrónico para Emisiones Conducidas de Banda Estrecha*
Tipo de participación: *Ponencia*
Congreso: *Congreso Nacional de la Unión Científica Internacional de Radio (URSI)*
Publicación: *CD de artículos*
Lugar de celebració: *Oviedo - España*
Fecha: *Septiembre 2006*

Autores: *D. Durán, J.R. Regué, M. Ribó, D. Badia, A. Pérez*
Título: *Caracterización modal de filtros de red a partir de parámetros S*
Tipo de participación: *Ponencia*
Congreso: *Congreso Nacional de la Unión Científica Internacional de Radio (URSI)*
Publicación: *CD de artículos*

Lugar de celebración: *Barcelona - España*
Fecha: *Septiembre 2004*

Characterization of Power-Line Filters and Electronic Equipment for Prediction of Conducted Emissions

Antonio Pérez, *Student Member*, *IEEE*, A.M. Sánchez, *Student Member*, *IEEE*, J.R. Regué, M. Ribó, *Senior Member*, *IEEE*, P. Rodríguez-Cepeda, *Student Member*, *IEEE*, F.J. Pajares, *Senior Member*, *IEEE*

***Abstract*—With present day standards and measurement techniques, it is very difficult to accurately predict the conducted interference levels of an electronic device connected to a power-line filter. In this paper, a new modal model (which takes into account common and differential mode interactions) for an electronic device is presented and tested. This model is used to develop a new methodology for the accurate prediction of the conducted emissions generated by a filtered electronic device. The modal point of view clarifies such phenomena as the loss of efficiency of power-line filters and the modal energy exchange due to mismatches and asymmetries in the circuits. This methodology allows an automatic software selection or design of the optimum power-line filter for a given electronic device. It has been successfully tested by using both test devices and actual electronic equipment.**

***Index Terms*— common mode, conducted emissions, conducted interference, differential mode, equivalent circuit, input impedance, power-line filter, power-line network, S parameters.**

I. Introduction

Current standards used to characterize power-line filters (PLF) [1] are based on separate phaseless measurements of the attenuation of the common and differential modes using 50 Ω line and load impedances. These characterizations do not allow the prediction of the behavior of a PLF in an actual environment because the actual line and load impedances are usually very different from 50 Ω ([2]-[3]), and they do not detect the fact that signals entering the filter as common or differential modes can be converted to the other mode by the PLF. These facts lead to an unpredictable decrease in the filter performance in an actual situation and to unexpected levels of conducted interference.

Several improvements to avoid these limitations can be found in the literature. In [4], a complete circuital characterization of a PLF, based on S-parameters, is presented. In [5], the mode conversion from common to differential modes is experimentally investigated. Finally, in [6], a technique based on time-domain measurements to find the optimal PLF for a given electronic device is presented.

Concerning the characterization of the conducted emissions of equipment under test (EUT), there are measurement techniques [7]-[8] that find the input impedance that the EUT presents to the common and differential modes. These techniques do not offer information neither about the interaction between common and differential modes that takes place in the EUT, nor about the conducted interference levels that the EUT injects to an arbitrary load connected to it.

Therefore, the present standards and measurement methods for PLFs and electronic devices are insufficient to accurately predict their combined conducted emission behavior. To solve this problem, the authors have been working to improve the joint characterization of PLFs and EUTs. In [9], a PLF is characterized by means of its S-parameters, both circuital (taking as its ports the line-ground and the neutral-ground ports) and modal (taking the common and the differential modes as excitations and responses). In [10]-[12] the electronic equipment input impedance (as seen from its power-line terminals) and the conducted interference that it generates are circuitally characterized using a three-impedance pi-network and two voltage sources.

In this paper, a new modal equivalent circuit (that takes into account common and differential mode signals instead of line-ground and neutral-ground ones) for a EUT is presented and tested. It consists of a three-impedance pi-network with two voltage sources, and improves the separate common mode and differential mode characterizations presented in [7]-[8]. This new modal model of the EUT, along with its circuital model described in [11], and the modal and circuital models for a PLF described in [9], is used to develop a new methodology for the prediction of the conducted emissions generated by a EUT with a PLF, connected to the power-line network or to a LISN. This new methodology can predict both the circuital (line and neutral) voltages and the modal (common and differential) voltages for any configuration of EUT, PLF, and power-line network. Therefore, the work presented in this paper is a useful tool to reduce the cost and the time duration for the optimum PLF selection or design, since it allows the prediction by software of interference levels in normative measurement set-ups from a series of previous easy-to-perform measurements.

Section II of this paper reviews the basics of the circuital and modal measurement of PLFs, and Section III.*A* the basics

This work has been funded by the projects TEC2004-02196 and TEC2005-04238 from the Spanish Ministerio de Educación y Ciencia.

of the circuital modeling of a EUT. In Section III.*B*, the new modal model for the generation of conducted emissions of a EUT is presented. In Section IV, the new methodology for predicting conducted emissions is presented. Section V presents the experimental validation of sections III.*B* and IV. Finally, the conclusions are presented in Section VI.

II. POWER-LINE FILTER CHARACTERIZATION

The electrical signals in the single-phase power-line terminals (line (L), neutral (N), and ground (G)) of any device can be characterized in two alternative ways (Fig. 1): circuitally (considering the physical voltages and currents V_L, V_N, I_L, I_N) and modally (electrical signals are decomposed into their common and differential modes, with voltages and currents V_{CM}, V_{DM}, I_{CM}, and I_{DM} respectively).

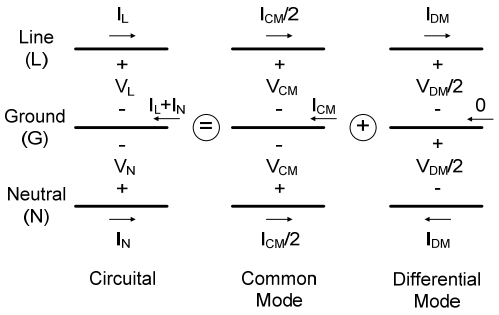

Fig. 1. Voltage and current definitions for the common and differential modes.

The relationship between circuital and modal voltages and currents are [13]:

$$V_{CM} = \frac{V_L + V_N}{2} \qquad I_{CM} = I_L + I_N$$
$$V_{DM} = V_L - V_N \qquad I_{DM} = \frac{I_L - I_N}{2}. \tag{1}$$

The S-parameters completely characterize the behavior of a linear RF circuit. Therefore, they can be used to characterize a PLF [9]. It can be modeled as a four-port network (Fig. 2(a)), with ports defined from line to ground (L-G ports) and from neutral to ground (N-G ports), where all the ports are referred to the physical ground (G). The circuital characterization of the PLF consists on the measurement of its S-parameter matrix, [S], using a measurement system with a reference impedance Z_0 (usually 50 Ω).

However, PLFs are best understood and analyzed considering their common and differential mode behavior. In order to obtain it, an equivalent circuit that relates the input and output common and differential modes has to be obtained (Fig. 2(b)). In this circuit, each mode is confined into a different port. All these ports are referred to a conceptual reference point whose relation with the physical ground is irrelevant for the purposes of this paper.

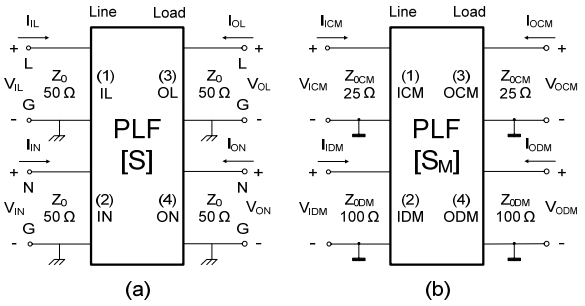

Fig. 2. Port definitions in a PLF. (a) Circuital. (b) Modal.

This equivalent circuit can be characterized [9] by a new S-parameter matrix, $[S_M]$, related to the circuital one by:

$$[S_M] = \frac{1}{2}\begin{bmatrix} 1 & 1 & 0 & 0 \\ 1 & -1 & 0 & 0 \\ 0 & 0 & 1 & 1 \\ 0 & 0 & 1 & -1 \end{bmatrix} \cdot [S] \cdot \begin{bmatrix} 1 & 1 & 0 & 0 \\ 1 & -1 & 0 & 0 \\ 0 & 0 & 1 & 1 \\ 0 & 0 & 1 & -1 \end{bmatrix} \tag{2}$$

In order to perform this transformation, the reference impedances must be $Z_{0CM}=Z_0/2$ for the common mode ports and $Z_{0DM}=2Z_0$ for the differential mode ports (Fig. 2(b)).

This is a more complete characterization than that of [1] since it takes into account reflections, phases, and the mode interchanges (between common and differential modes). Besides, it is able to predict the behavior of the PLF connected to any line and load impedances.

III. ELECTRONIC DEVICE CHARACTERIZATION

A. Circuital Characterization

In [11], an electronic device, which can be considered reciprocal as seen from its power-line terminals, is modeled by a three-impedance network with two voltage sources connected to the line and neutral terminals (Fig. 3). This circuit, among others [14]-[15], completely characterizes the behavior of the conducted interferences generated by any electronic device. The structure of Fig. 3 has been chosen for its simplicity of interpretation.

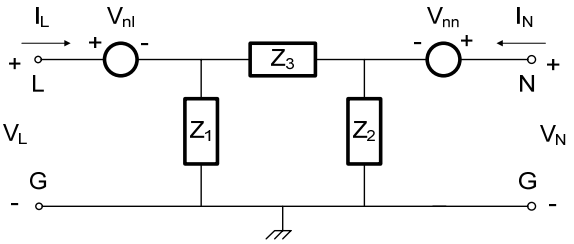

Fig. 3. Circuital model for an electronic device.

The values of the impedances Z_1, Z_2, and Z_3 are found from S-parameter measurements (the port 1 is the L-G port and the

port 2 is the N-G one):

$$Z_1 = \frac{Z_o\left(1+S_{11}\right)\left(1+S_{22}\right)-Z_oS_{12}S_{21}}{\left(1-S_{11}\right)\left(1+S_{22}\right)+S_{12}S_{21}-2S_{21}}$$
$$Z_2 = \frac{Z_o\left(1+S_{22}\right)\left(1+S_{11}\right)-Z_oS_{21}S_{12}}{\left(1-S_{22}\right)\left(1+S_{11}\right)+S_{21}S_{12}-2S_{12}} \quad (3)$$
$$Z_3 = \frac{Z_o\left(1+S_{11}\right)\left(1+S_{22}\right)-Z_oS_{12}S_{21}}{S_{12}+S_{21}},$$

where Z_0 is the reference impedance of the measurement system (Fig. 4), which basically consists of a network analyzer and a Line Impedance Stabilizing Network (LISN) [10]. To obtain a correct S-parameter measurement, the power of the interference generated by the EUT has to be negligible in front of the power delivered by the vector network analyzer [12]. The LISN presents a high isolation between the power-line ports (L_{PL}-G and N_{PL}-G) and the rest of the ports at the conducted emission range, so the effect of the power-line network impedance is negligible in the measurement. In order to achieve a good frequency response (only limited by the LISN frequency response), the L-G-N terminals of the LISN and the EUT have been converted into two coaxial lines: their inner conductors correspond to the line and neutral terminals, and their outer conductors to the ground.

In order to compensate the effects of the LISN, the transient limiters, and the cables, the system is calibrated at the LISN-EUT interface using a standard TOSM (Through-Open-Short-Match) vector network analyzer calibration method.

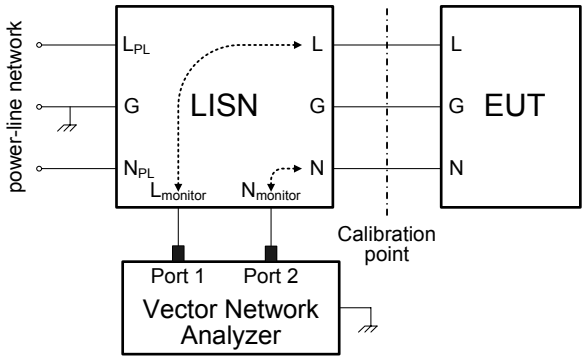

Fig. 4. Block diagram of the S-parameter measurement system.

In order to find the values of the two voltage sources (V_{nl}, V_{nn}), it suffices to apply Kirchoff laws to the circuital model of Fig. 3 and to measure the voltages and currents at the terminals of the EUT (V_L, I_L, V_N, I_N) as defined in Fig. 5:

$$V_{nl} = V_L - \frac{Z_1\left(Z_2+Z_3\right)I_L + Z_1Z_2I_N}{Z_1+Z_2+Z_3}$$
$$V_{nn} = V_N - \frac{Z_2\left(Z_1+Z_3\right)I_N + Z_1Z_2I_L}{Z_1+Z_2+Z_3}. \quad (4)$$

The set-up used to measure the voltages and currents at the terminals of the EUT (Fig. 5) consists of a two-port vector spectrum analyzer (a vector network analyzer can be used if its receivers are accessible), and a LISN. The values of V_L, I_L, V_N, and I_N are obtained from the measured values V_{BL} and V_{BN}, compensating the effect of the LISN as described in [11].

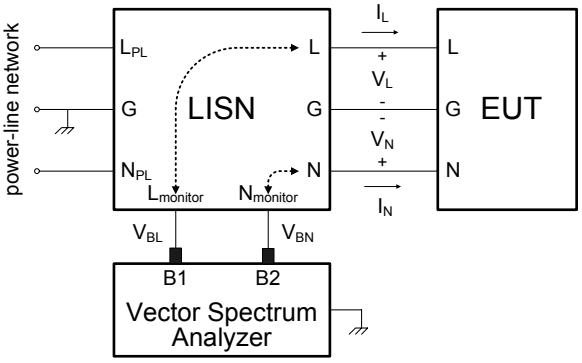

Fig. 5. Block diagram of the measurement system of the voltages and currents at the terminals of the EUT.

The circuit model thus obtained is a more complete representation of the conducted emission behavior of a EUT than the traditional measurement following the standards [16] because it takes into account not only the level of the interfering line and neutral signals, but also their phase, and the complete impedance behavior of the EUT.

B. Modal Characterization

The circuital model summarized above allows a characterization of a EUT, but it gives no clue as to its behavior as a common mode and differential mode conducted interference generator. A model in terms of common and differential impedances and sources of interference (a modal model, Fig. 6) is more interesting in order to analyze its behavior, since the analysis from a modal point of view allows a better interpretation of the interference generation and propagation phenomena. The model of Fig. 6, which has the structure of a generic two-port device with inner sources, consists of a three-impedance pi-network (the common mode impedance Z_{CM}, the differential mode impedance Z_{DM}, and the modal transimpedance Z_{TM}, which accounts for interactions between the common and differential modes in the EUT) and two series voltage sources (V_{nCM} and V_{nDM}), which model the generation of common and differential mode conducted interferences by the EUT, respectively. As can be seen, this modal model splits either mode generated by the EUT into a different port (namely, a common mode port and a differential mode port), and allows a simple interpretation of usual situations in which either mode behaves in a different way. In particular, this modal model will allow the evaluation of the complete behavior of a PLF connected to the EUT (common and differential mode insertion losses and energy exchange

between modes).

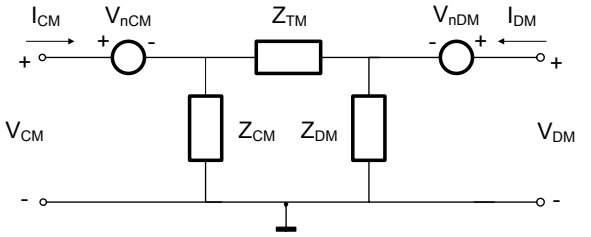

Fig. 6. Modal model for an electronic device.

The parameters of the modal model of Fig. 6 can be derived from the existing relationship between the circuital voltages and currents (V_L, I_L, V_N, I_N) and the modal ones (V_{CM}, I_{CM}, V_{DM}, I_{DM}). By combining (1) and (4), the modal currents I_{CM}, I_{DM} are obtained:

$$\begin{aligned} I_{CM} &= \left(\frac{1}{Z_1}+\frac{1}{Z_2}\right)V_{CM}+\left(\frac{1}{2Z_1}-\frac{1}{2Z_2}\right)V_{DM}-\frac{V_{nl}}{Z_1}-\frac{V_{nn}}{Z_2} \\ I_{DM} &= \left(\frac{1}{2Z_1}-\frac{1}{2Z_2}\right)V_{CM}+\left(\frac{1}{4Z_1}+\frac{1}{4Z_2}+\frac{1}{Z_3}\right)V_{DM}- \\ &-\left(\frac{1}{2Z_1}+\frac{1}{Z_3}\right)V_{nl}+\left(\frac{1}{2Z_2}+\frac{1}{Z_3}\right)V_{nn}\,. \end{aligned} \tag{5}$$

By analyzing the circuit of Fig. 6 the following equations are obtained:

$$\begin{aligned} I_{CM} &= \left(\frac{1}{Z_{CM}}+\frac{1}{Z_{TM}}\right)V_{CM}-\frac{1}{Z_{TM}}V_{DM}- \\ &-\left(\frac{1}{Z_{CM}}+\frac{1}{Z_{TM}}\right)V_{nCM}+\frac{1}{Z_{TM}}V_{nDM} \\ I_{DM} &= -\frac{1}{Z_{TM}}V_{CM}+\left(\frac{1}{Z_{DM}}+\frac{1}{Z_{TM}}\right)V_{DM}+ \\ &+\frac{1}{Z_{TM}}V_{nCM}-\left(\frac{1}{Z_{DM}}+\frac{1}{Z_{TM}}\right)V_{nDM}\,. \end{aligned} \tag{6}$$

By comparing (5) and (6), the values of Z_{CM}, Z_{DM}, Z_{TM}, V_{nCM}, and V_{nDM} are derived:

$$\begin{aligned} Z_{CM} &= \frac{2Z_1Z_2}{Z_1+3Z_2} \\ Z_{DM} &= \frac{4Z_1Z_2Z_3}{4Z_1Z_2+3Z_2Z_3-Z_1Z_3} \\ Z_{TM} &= \frac{2Z_1Z_2}{Z_1-Z_2}\,. \end{aligned} \tag{7}$$

$$\begin{aligned} V_{nCM} &= \frac{V_{nl}+V_{nn}}{2} \\ V_{nDM} &= V_{nl}-V_{nn}\,. \end{aligned} \tag{8}$$

As can be seen from (7), when the EUT is unbalanced ($Z_1 \neq Z_2$), the modal transimpedance Z_{TM} takes a finite value, causing an energy transfer between common and differential modes (for instance, an incident common mode to the EUT can be reflected as both a common and a differential mode). This fact shows that the common and differential mode impedances are not enough to model the behavior of a EUT concerning common and differential mode generation and behavior: it cannot be modeled as two isolated generators (one for the common mode with source impedance Z_{CM}, and another one for the differential mode with source impedance Z_{DM}), but has to be considered as the more complex circuit of Fig. 6. Therefore, the characterization described above improves on previous ones that consider the common mode and differential mode behavior of a EUT as isolated phenomena [7]-[8].

Although it is not obvious from equations (5) and (6), V_{nCM} and V_{nDM} have the same form as the definitions of voltages for the common and differential modes of (1). This fact shows that the only source of energy exchange between common and differential modes at any EUT is the modal transimpedance (Z_{TM}).

IV. PREDICTION OF THE CONDUCTED EMISSIONS USING EQUIVALENT MODELS

Once models for the EUT and the PLF are available (both circuital and modal), they can be applied to the prediction of the circuital voltages (at the L-G and N-G ports) and the modal voltages (for the common and differential modes) at the Line-side of the PLF. This fact will allow an optimum selection or design of the PLF for a given EUT since the resultant values of interference can be computed for any load conditions.

A. Circuital Simulation of a EUT with a PLF

To perform a circuital prediction of the conducted interference levels generated by a EUT with a PLF, the following steps must be followed:

1. Circuital characterization of the PLF as described in Section II.
2. Circuital characterization of the EUT as described in Subsection III.*A*.
3. Circuital characterization of the power-line network as explained below.
4. Combined simulation of the previous models using a circuit simulator or by direct programming of the equations. Fig. 7 shows the elements used in the circuital simulation: the circuit models for the EUT, the PLF, and the power-line network. The circuital simulation has to obtain the voltages V_L and V_N.

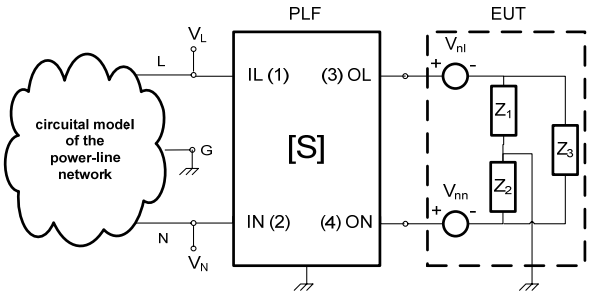

Fig. 7. Circuital simulation of a EUT with a PLF.

The circuital model for the power-line network of Fig. 7 can be any of the listed below:

1. A LISN nominal impedance model (i.e. 50 Ω || 50 μH if an emulation of the measurement according to standard [17] is desired, Fig. 8(a)). This model is interesting for comparing the conducted interference levels at the Line-side terminals of the PLF with the levels established by EMC standards such as [16].
2. The actual circuital S-parameters of the LISN used in an eventual measurement (Fig. 8(b)). They can be measured using the procedure described in Section II. In order to characterize a LISN as a four port device, its power-line ports (L_{PL}-G and N_{PL}-G) are not considered since they are largely isolated and the actual power-line network does not affect the measurements. In the simulation, the measurement ports of the LISN ($L_{monitor}$–G and $N_{monitor}$–G) are loaded with 50 Ω. This modeling of the power-line network is more precise than the previous one, since it considers the parameters of the actual LISN used in the measurement system.

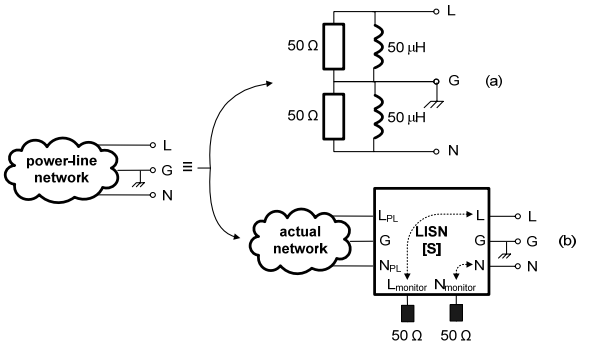

Fig. 8. Equivalent circuital models for the power-line network. (a) Nominal impedance LISN model. (b) Real LISN model.

B. Modal Simulation of a EUT with a PLF

To perform a modal prediction of the conducted interference levels generated by a EUT with a PLF (common and differential mode voltages at the Line-side of the PLF) the following steps must be followed:

1. Modal characterization of the PLF as described in Section II.
2. Modal characterization of the EUT as described in Subsection III.*B*.
3. Modal characterization of the power-line network. It is obtained from the circuital characterization described in the Subsection IV.*A* using the mathematical transformation procedures presented in Sections II for the model of Fig. 8(b) and III for the model of Fig. 8(a).
4. Combined simulation of the previous models using a circuit simulator or by direct programming of the equations. Fig. 9 shows the elements used in the modal simulation: the modal models for the EUT, the PLF, and the power-line network. The modal simulation has to obtain the voltages V_{CM} and V_{DM}.

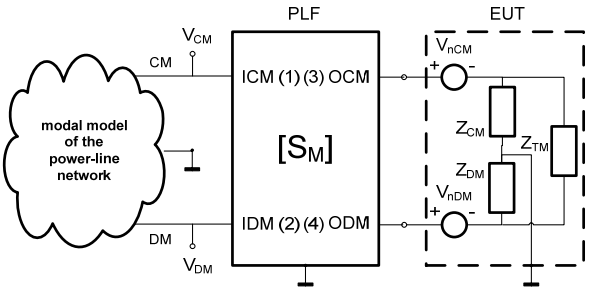

Fig. 9. Modal simulation of a EUT with a PLF.

Since the whole system is modally modeled, it is possible to identify qualitatively but also quantitatively how interferences behave. For instance, if there is a mismatch between the output common mode generated by the EUT and the port OCM (3) of the PLF, this mode will be reflected back to the EUT. If the EUT has a low modal transimpedance Z_{TM}, it will convert part of this reflected common mode into the differential mode, varying the amount of the differential mode conducted emissions. Therefore, this modal modeling can explain, for instance, how a mismatch in the filter for the common mode can lead to an increase of the conducted emissions for the differential mode.

V. EXPERIMENTAL RESULTS

In order to validate the modal model for a EUT and the circuital and modal methodologies for the prediction of conducted interferences, two electronic devices (a test device and a commercial HF transceiver) have been measured and modeled, and their conducted interference levels predicted when connected to a PLF.

A. Test Device

The test device of Fig. 10 has been built in order to test the models and methodologies proposed in this paper. The voltage sources V_{nl}' and V_{nn}' have been implemented using an RF generator with two outputs of equal amplitude (97 dBμV) and a phase-shift between them of 53º. The generator sweeps the frequency range from 50 kHz to 35 MHz. The 50 Ω inner impedances of the RF generator (Z_{gl}' and Z_{gn}') have been

included to the impedances Z_1' and Z_2' of the circuit.

1) Verification of the modal model

Since the inner structure of the test device is known, it can be used to validate the modal model proposed in Subsection III.*B*. Indeed, any of its circuital and modal parameters can be analytically computed from the theory described in the previous sections. Therefore, the adequacy of the modal model of a EUT can be put to the test. In order to do so, the modal parameters of the circuit (Z_{CM}, Z_{DM}, Z_{TM}, V_{nCM}, and V_{nDM}, see Fig. 6) will be obtained from real measurements, and compared to those computed analytically from its inner structure.

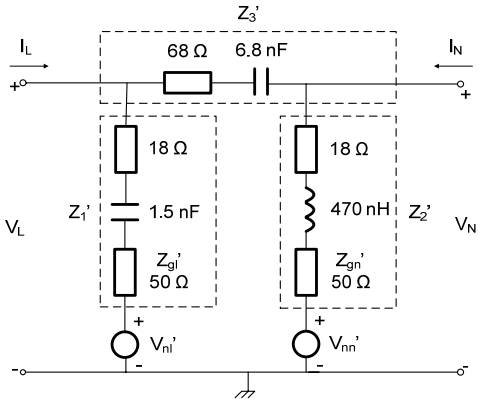

Fig. 10. Test device.

Fig. 11 shows the comparison between the computed and the measured values for the modal impedances for the test device of Fig. 10. Fig. 12 shows the comparison between the computed and the measured values for the modal voltages V_{nCM} and V_{nDM}. The good agreement between computation and measurement validates the modal model, and also validates the measurement system.

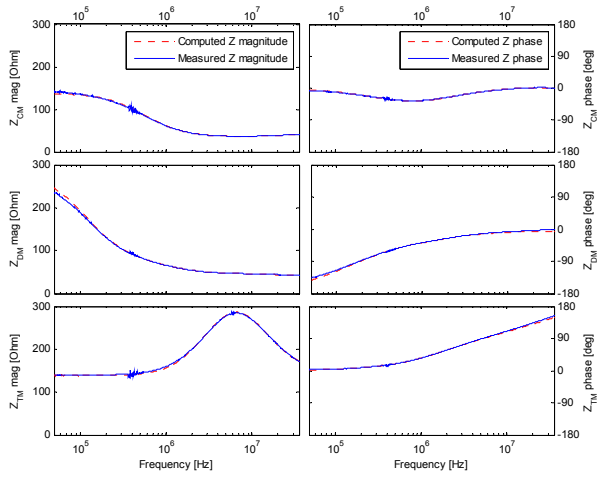

Fig. 11. Comparison between measured and computed Z_{CM}, Z_{DM}, and Z_{TM} impedances of the modal model for the test circuit of Fig. 10.

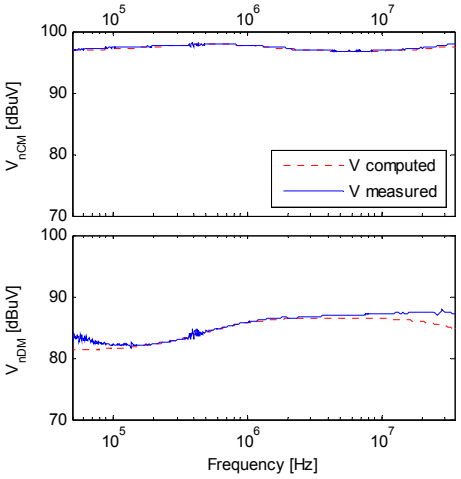

Fig. 12. Comparison between measurement and computation for the interference voltage sources V_{nCM} and V_{nDM} of the modal model for the test device of Fig. 10.

2) Prediction of the circuital and modal voltages of the test device with a PLF

Once the circuital and modal models of the test device are known (the parameters of the circuital model are not shown above), they can be used to predict the values of the conducted interference after being filtered by a PLF in a variety of situations, as described in Section IV. To test the viability of this new approach, a PLF (Fig. 13, with values R = 10 MΩ, L = 1.8 mH, C_Y = 3.5 nF, C_X = 100 nF) has been connected to the test device of Fig. 10.

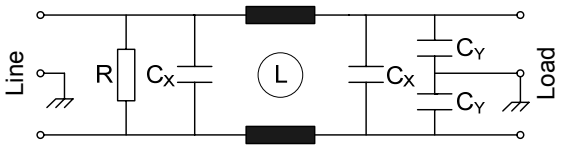

Fig. 13. Schematic of the power-line filter.

The resulting circuit has been measured using the measurement set-up of Fig. 14.

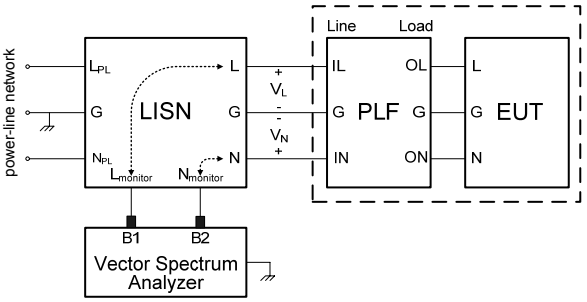

Fig. 14. Block diagram for the measurement set-up of the voltage in the line terminals of the test device with a PLF.

Fig. 15 compares the predicted (as described in Section IV.*A*) and measured values of V_L and V_N (their magnitudes

and their relative phase), showing very good agreement.

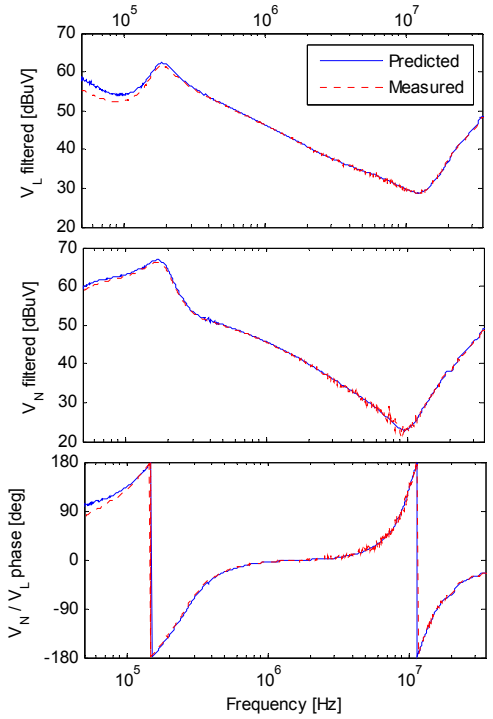

Fig. 15. Predicted and measured circuital voltages V_L and V_N for the configuration of Fig. 14.

Once the circuital voltages (V_L and V_N) have been measured, by using (1) the common and differential voltages (V_{CM} and V_{DM}) are obtained at the Line-side of the PLF. These values are also predicted using the approach described in Section IV.*B* (in this case using the modal models instead of the circuital ones).

Fig. 16 compares the measured and predicted values of V_{CM} and V_{DM}, showing again a very good agreement.

The good agreement between prediction and measurement validates both circuital and modal proposed methodologies.

In order to state the importance of a complete modal characterization of the EUT, a prediction of the modal conducted emissions generated by the filtered EUT has been made, but this time with $Z_{TM} = \infty$ to emulate a characterization of the EUT considering only its common and differential mode impedances. Since there is no connection between common and differential modes at the EUT, the reflections of the conducted emissions at the Load-side ports of the PLF (due to mismatches between the common and differential mode input impedances of the PLF and those of the EUT) that return to the EUT are not converted to the other mode by Z_{TM}, as happens in the actual device. Table 1 compares, at two selected frequencies, the measured levels of common and differential mode interference at the Line-side of the PLF with the simulated ones with a EUT with $Z_{TM} = \infty$. As can be seen, the predicted values do not match the measured ones. This fact shows that in the design of an optimum PLF for a given EUT, its whole modal model has to be considered in order to account for all the modal conversions that can degrade its behavior. As can be seen in this example, not only the inner mode conversion at the components of the PLF can degrade its performance, but also the interactions (originated by mismatches) of the PLF with mode conversion mechanisms at the components of the EUT.

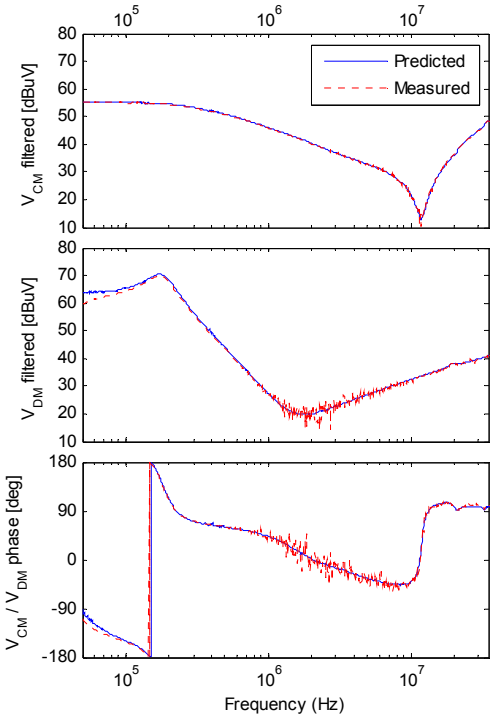

Fig. 16. Predicted and measured modal voltages V_{CM} and V_{DM} for the configuration of Fig. 14.

Table 1. Comparison Between Measurement and Prediction with $Z_{TM} = \infty$.

Frequency [KHz]	Measured V_{CM} [dBμV]	Predicted V_{CM} [dBμV]	Measured V_{DM} [dBμV]	Predicted V_{DM} [dBμV]
176.7	54.76	52.36	69.89	63.02
300.0	53.26	50.11	55.94	49.38

3) Comparison with predictions made using present day standards

As stated in the introduction, present day standards used to characterize PLFs [1] are of little use when line and load impedances are not 50 Ω. Besides, they do not detect the modal conversion between modes in the PLF. These facts lead to an unexpected decrease in the performance of the filter.

It is, however, a common practice among EMC engineers to compute the expected values of conducted emissions of a EUT with a PLF simply by substracting from the conducted emissions generated by the EUT (without the PLF) the values of the common and differential mode attenuations of the PLF as measured by the standards. Fig. 17 compares the predicted common and differential mode voltages according to this

common practice with the actual measured values. As can be seen, the error can be significant, in contrast to the results obtained using the method described in this paper (Fig. 16). This fact corroborates the adequacy of the approach adopted in this paper to predict conducted emissions.

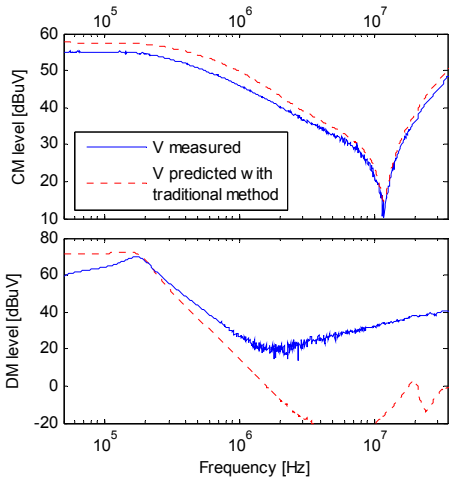

Fig. 17. Comparison between the conducted emissions predicted according to the common engineering practice and the measured ones.

B. *Commercial HF Transceiver*

The models and methodologies proposed in this paper have been applied to a commercial 100 W HF transceiver transmitting a 4 MHz carrier, in order to test their adequacy with actual devices.

Concerning the prediction of the conducted emission levels, the whole process has been applied to the HF transceiver:

1. Its circuital and modal models have been derived from measurements.
2. The circuital S-parameters of the desired PLF (Fig. 13, with values R = 1 MΩ, L = 4.6 mH, C_X = 33 nF, C_Y = 0) have been measured, and the modal ones computed.
3. The circuit has been measured using the same measurement set-up used in the previous example (Fig. 14), obtaining both the circuital and modal filtered conducted emissions (V_L, V_N, V_{CM}, and V_{DM}).
4. The voltages (V_L, V_N, V_{CM}, and V_{DM}) have been predicted using the methodology of Section IV.

Fig. 18 and Fig. 19 compare the measured and predicted values of the magnitudes of V_L and V_N, and V_{CM} and V_{DM}, respectively. A set of interferences in the band from 150 kHz to 2 MHz, generated by the switching power supply of the transceiver, can be seen. Interferences at multiple frequencies of 4 MHz are also noticeable. Measured interference levels below 10 dBμV are masked by the noise floor level of the measurement system. The very good agreement between measurement and prediction validates the approach presented in this paper, and shows that it is possible to predict the levels of conducted emissions that a generic EUT loaded with a PLF generates according to the desired standard [16].

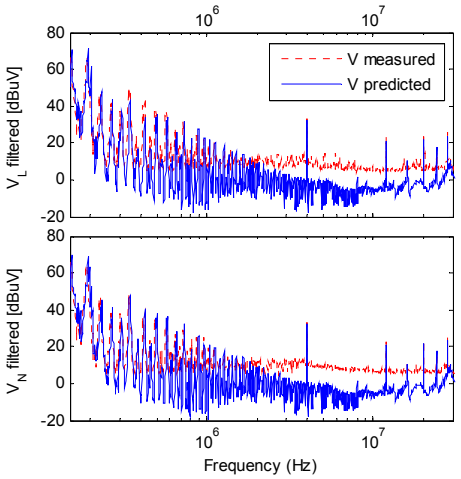

Fig. 18. Predicted and measured circuital voltages V_L and V_N for the HF transceiver.

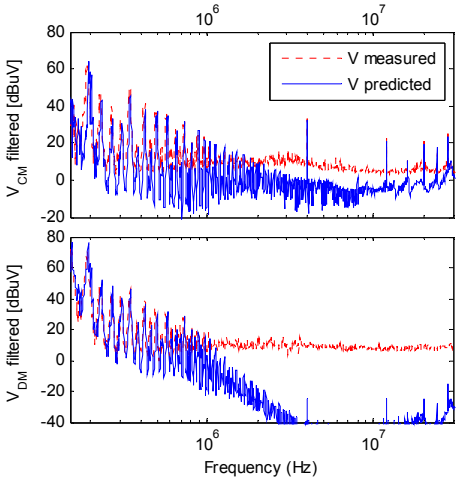

Fig. 19. Predicted and measured modal voltages V_{CM} and V_{DM} for the HF transceiver.

This approach can be very useful in the design of an electronic device, since its levels of conducted emissions can be easily predicted when loaded with previously measured PLFs. This way, long and costly sessions of filter-assembly and measurement can be avoided: the EUT has to be measured once (in order to obtain its circuital and modal models), and its behavior when connected to a set of previously measured filters (as described in Section II) easily and rapidly predicted using the methodology of Section IV.

As in the previous example, the predictions made by the method described in this paper have been compared to the predictions made using the PLF attenuations given by the present standards. For most of the common mode interfering frequencies, errors of the order of 15 dB have been observed.

VI. CONCLUSIONS

In this paper, a new modal model for characterizing an electronic device as a conducted interference generator (as seen from its power-line terminals) has been presented and tested. This modal model splits the contributions of each conducted interfering mode (the common and the differential modes) into a different port. Therefore, it is useful to analyze the frequent situations in which either mode behaves in a different way: for instance, when a power-line filter is connected to the electronic device, since it presents different attenuation and matching to each mode. The derived model is complete since it takes into account both the impedance behavior of the electronic equipment and its interference sources. It is also more precise than separate common mode-differential mode characterizations because it takes into account inner energy transfers between common and differential modes, modeled by a modal transimpedance Z_{TM}. This model has been experimentally validated.

This new model, along with the other models summarized in this paper, has been used to develop a new methodology for the accurate prediction of the conducted emissions of an electronic device, after being filtered by a power-line filter, according to the desired standards (i.e. CISPR 22). Its relevant features are:

- It allows the computation of the actual common and differential mode attenuation of a power-line filter in a real situation (for instance, a filter connected to an electronic device and to a LISN).
- It can lead to a selection (or design) by software of a filter optimally adapted to the actual electronic equipment avoiding a costly trial-and-error filter selection process. Besides, the filters need not to be over specified to compensate for impedance mismatches, modal conversion, etc.
- It allows the prediction of effects such as the modal conversion, from common to differential mode and vice versa, generated by asymmetries in the components of a power-line filter, or by modal transimpedances in the electronic device.

The methodology presented in this paper brings a complete solution to the analysis of the conducted interferences of electronic equipment with a power-line filter. It betters the results predicted using measurements performed according to present standards, with even simpler measurement techniques and set-ups. Therefore, it can be very useful to power-line filter manufacturers, as well as to electronic equipment designers and to EMC laboratories.

REFERENCES

[1] ANSI C63.13, *American National Standard Guide on the Application and Evaluation of EMI Power-Line Filters for Commercial Use*, American National Standards Institute, June 28, 1991.

[2] B. Garry and R. Nelson, "Effect of impedance and frequency variation on insertion loss for a typical power line filter", *Proc. of IEEE Symp. on EMC*, Aug. 24-28, 1998, pp. 691-695.

[3] M. Zamazal and T. Urbanec, "Variable impedance in measuring EMI filter's insertion loss", *Asia-Pacific Conf. on Communications*, Oct. 3-5, 2005, pp. 24-27.

[4] J.G. Kraemer, "S-parameter characterization for EMI filters", *Proc. of IEEE Symp. on EMC*, Aug. 18-22, 2003, pp. 361-366.

[5] A. Axelrod, "Experimental study of DM-to-CM and vice-versa conversion effects in balanced signal and power line filters", *Proc. of IEEE Symp. on EMC*, May 11-16, 2003, pp. 599-602.

[6] M. Kumar and V. Agarwal, "Power line filter design for conducted electromagnetic interference using time-domain measurements", *IEEE Trans. Electromagn. Compat.*, Feb., 2006, Vol. 48, No. 1, pp. 178-186.

[7] K.Y. See and L. Yang, "Measurement of noise source impedance of SMPS using two current probes", *IEE Electronic Letters*, Oct., 2000, Vol. 36, No. 21, pp. 1774-1776.

[8] D. Zhang, D.Y. Chen, M.J. Nave, and D. Sable, "Measurement of noise source impedance of off-line converters", *IEEE Trans. on Power Electronics*, Sept., 2000, Vol. 15, No. 5, pp. 820-825.

[9] J.R. Regué, M. Ribó, D. Duran, D. Badia, and A. Pérez, "Common and differential mode characterization of EMI power-line filters from S-parameters measurements", *Proc. of IEEE Symp. on EMC*, Aug. 9-13, 2004, Vol. 2, pp. 610-615.

[10] J.R. Regué, M. Ribó, D. Duran, D. Badia, and A. Pérez, "Measurement and modeling of noise source impedance of electronic equipment", *Proc. of the 6th EMC Europe Int. Symp.*, Sept. 6-10, 2004, Eindhoven, The Netherlands, pp. 150-154.

[11] A. Pérez, J.R. Regué, M. Ribó, A.M. Sánchez, F.J. Pajares, and D. Badia, "Circuital characterization of an electronic equipment for narrow-band conducted emissions", *Proc. of the 7th EMC Europe Int. Symp.*, Sept. 5-8, 2006, Barcelona, Spain, pp. 1035-1040.

[12] A.M. Sánchez, A. Pérez, J.R. Regué, M. Ribó, P. Rodríguez-Cepeda, and F.J. Pajares, "Optimization of the scattering parameter measurement of electronic equipment with conducted emissions", *CD of Proc. of EMC Europe Workshop*, June 14-15, 2007, Paris, France.

[13] H.L. Su and K.H. Lin, "Computer-aided design of power line filters with a low cost common and differential-mode noise diagnostic circuit", *Proc. of IEEE Symp. on EMC*, Aug. 13-17, 2001, pp. 511-516.

[14] D.M. Pozar, *Microwave Engineering*, John Wiley & Sons, Inc., USA, 1998.

[15] H. Rothe, W. Dahlke, "Theory of noisy fourpoles", *Proc. of the IRE*, June, 1956, pp. 811-818.

[16] CISPR 22, *Information Technology Equipment—Radio Disturbance Characteristics—Limits and Methods of Measurement*, International Electrotechnical Commission, Nov., 1997.

[17] CISPR 16, *Specification for Radio Disturbance and Immunity Measuring Apparatus and Methods*, International Electrotechnical Commission, Nov., 2003.

OPTIMIZATION OF THE SCATTERING PARAMETER MEASUREMENT OF ELECTRONIC EQUIPMENT WITH CONDUCTED EMISSIONS

A.M. Sánchez, A. Pérez, J.R. Regué, M. Ribó, P. Rodríguez-Cepeda, F.J. Pajares
GRECO – Grup de Recerca en Electromagnetisme i Comunicacions
Enginyeria i Arquitectura La Salle
Universitat Ramón Llull
Quatre Camins 2, 08022 Barcelona (Spain)
E-mail: albertm@salle.url.edu, antonip@salle.url.edu, jramon@salle.url.edu, mrp@salle.url.edu, jprodriguez@salle.url.edu, fpajares@salle.url.edu

Abstract: This paper presents two new measurement methods useful to obtain a better characterization of the input impedance of electronic equipment connected to the power line. This characterization is performed using a three-impedance pi-model network, which is obtained from an S-parameter measurement of the equipment. Both methods proposed in this paper improve the accuracy of S-parameter measurements, and consequently yield more accurate equivalent models. The knowledge of these models is very useful to design and/or to choose the most suitable power-line filter, since they allow an accurate prediction of the filter attenuation in common and differential modes. These new techniques are experimentally tested using real measurements.

I. INTRODUCTION

The present standards used to characterize power line-filters ([1], [2]), are based on measurements of common and differential mode attenuation with line and load impedances of 50 Ω. Those methods do not work properly to predict the filter behaviour in a real environment, where the impedances may be different from 50 Ω.

In [3], a power-line filter is characterized by means of its S-parameters, physical (line and neutral terminals) and modal (common and differential mode). To make this characterization useful in a design context, a similar characterization for the electronic equipment, that considers either its physical ports (line-ground and neutral-ground) or its modal equivalents (common and differential) must be employed.

In [4] and [5], a full model is presented (using physical and modal ports) to characterize the electronic equipment input impedance (seen from the power line terminals). The equipment is characterized using a three equivalent impedance pi-model, which is obtained from the S-parameter measurements. From this circuital model, a new equivalent modal model is obtained. The modal model can predict the real attenuation of a power line filter connected to the electronic equipment.
This paper presents two new measurement methods to obtain the S-parameters of electronic equipment connected to the power-line. These methods improve the previous proposals presented in [4] and [5]. A more accurate S-parameter measurement will allow a better characterization of the EUT (Equipment Under Test) by means of its equivalent circuital and modal models.

II. EQUIVALENT CIRCUITAL MODEL OF A EUT

The three terminals of the power-line of a EUT can be analyzed as a two port network (Fig. 1). The port "L" is defined between the line terminal and the ground terminal, and the port "N" is defined between the neutral terminal and the ground terminal.

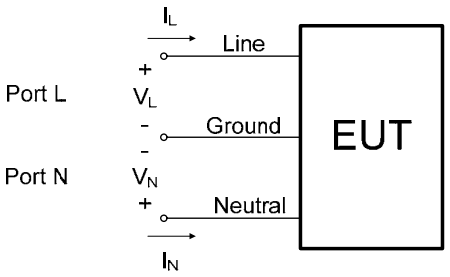

Fig. 1. EUT port definition.

Assuming that this network is reciprocal, it can be modeled using a pi-network [6] (Fig. 2).

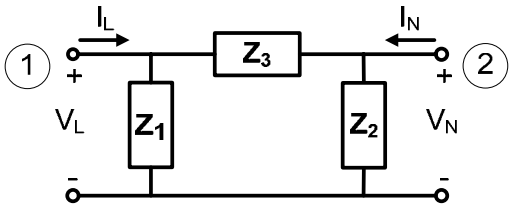

Fig. 2. Circuital model of three impedances in pi.

The value of the three impedances (Z_1, Z_2 and Z_3) of the circuital model of Fig. 2 can be found from the S-parameter measurements at both ports of the EUT [5]:

$$Z_1 = \frac{Z_o(1+S_{11})(1+S_{22}) - Z_o S_{12}S_{21}}{(1-S_{11})(1+S_{22}) + S_{12}S_{21} - 2S_{21}}$$
$$Z_2 = \frac{Z_o(1+S_{11})(1+S_{22}) - Z_o S_{12}S_{21}}{(1+S_{11})(1-S_{22}) + S_{12}S_{21} - 2S_{21}} \quad (1)$$
$$Z_3 = \frac{Z_o(1+S_{11})(1+S_{22}) - Z_o S_{12}S_{21}}{2S_{21}}$$

where Z_o is the reference impedance of the measurement system, the port 1 is the "L" port and the port 2 is the "N" port.

III. LIMITATIONS OF THE PRESENT S-PARAMETER MEASUREMENT SYSTEM

The configuration used to measure the S-parameter of the EUT (Fig. 3) consists of a network analyzer and a coupling network (LISN: Line Impedance Stabilizing Network) [4].

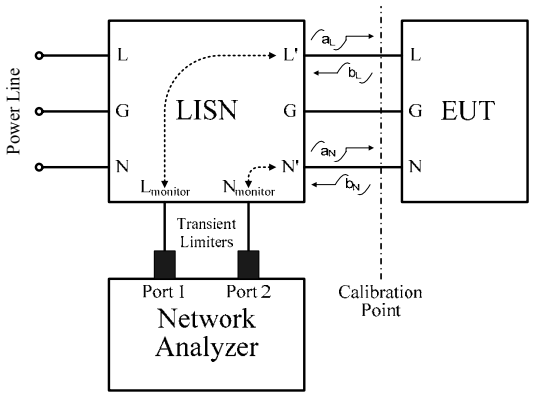

Fig. 3. Block diagram of the measurement system.

In order to compensate the effect produced by the LISN, the transient limiters and the interconnection cables in the S-parameter measurement of the EUT, the standard calibration procedure of the network analyzer is performed considering the ports of the LISN that are connected to the EUT as the calibration ports.

This measurement configuration has the following limitations:

- To obtain a correct S-parameters measurement, the interference generated by the EUT has to be negligible in front of the power delivered by the network analyzer. Otherwise, the reflected or transmitted wave by the EUT can be masked by its own interference.
- Not all the network analyzers can be calibrated using the method proposed in Fig. 3, because of the transient limiter attenuation, of approximately 10 dB, connected between the measurement ports (LISN terminals connected to the EUT) and the network analyzer ports. Furthermore, the LISN introduces a big attenuation at low frequencies, and it has to be compensated as well.

This paper proposes, keeping the initial set-up, two new techniques in the measurement process that improve the limitations presented above:

- Interpolation: this method allows using network analyzers without a high output power, ensuring the S-parameter measurement integrity.
- Deembedding: this method extracts the S-parameters of the EUT mathematically, when the network analyzer is calibrated on its own ports, instead on the LISN ports that are connected to the EUT.

IV. SOLUTIONS PROPOSED

IV.1 Interpolation

The interpolation method corrects the S-parameter measurements at those frequencies where the interference level generated by the EUT exceeds the risk threshold for the measurement integrity. To decide if a frequency is over this threshold, two measurements have to be performed:

- Interference level generated by the EUT [dBμV] on its line and neutral ports at the operation frequencies where the S-parameter measurement will be done. The output power of the network analyzer has to be zero ($a_L = a_N = 0$).
- Level of the b_L and b_N waves [dBμV] in the measurement ports using the configuration of Fig. 3, where the interference generated by the EUT is mixed with the reflected wave due to the input impedance of the EUT. In this case the network analyzer is supplying its nominal power (a_L, $a_N \neq 0$).

If the second measurement is under a threshold level added to the first measurement, it can be considered that the interference of the EUT will affect the measurement, so the S-parameter measurement must be corrected at that frequency. To correct the S-parameter at a particular operation frequency it is only necessary to find the two nearest frequencies without interferences and perform a lineal interpolation of the S-parameter. The section V of this paper (experimental validation) shows some measurements of real equipment that validate the correct performance of this method.

IV.2 Deembedding

The deembedding method compensates, by means of analytical computations, the effect caused by the LISN, the transient limiters and the interconnection cables in the EUT S-parameter measurement, when the calibration is performed directly on the network analyzer ports instead on the LISN ports connected to the EUT. The Fig. 4 groups those elements and presents them as a two and four port network.

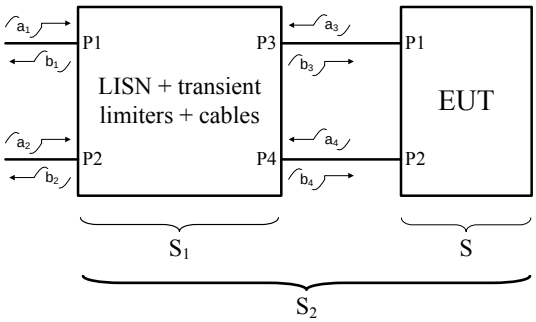

Fig. 4. Port definition of the measurement system.

To find the S-parameter of the EUT (S) it is necessary to have previously measured:

- S-parameter of the set LISN + transient limiters + cables (S_1).
- S-parameter of the set LISN + transient limiters + cables + EUT (S_2).

The S-parameter matrix links the output waves *b* with the input waves *a* of each port of the EUT [4]:

$$\begin{bmatrix} a_3 \\ a_4 \end{bmatrix} = [S] \cdot \begin{bmatrix} b_3 \\ b_4 \end{bmatrix} \tag{2}$$

To find the S-parameter matrix of the EUT it is necessary to express a_3 and a_4 in function of b_3 and b_4, and this will be achieved thanks to the S_1 and S_2 matrix:

$$\begin{bmatrix} b_1 \\ b_2 \\ b_3 \\ b_4 \end{bmatrix} = [S_1] \cdot \begin{bmatrix} a_1 \\ a_2 \\ a_3 \\ a_4 \end{bmatrix} \tag{3}$$

$$\begin{bmatrix} b_1 \\ b_2 \end{bmatrix} = [S_2] \cdot \begin{bmatrix} a_1 \\ a_2 \end{bmatrix} \tag{4}$$

In [7] [8], a mathematical method to extract the coefficients of the S-parameter matrix of the EUT from the known matrixes S_1 and S_2 is presented:

$$\begin{aligned} S_{11} &= \frac{DE - CF}{AD - BC} \;;\; S_{12} = \frac{AF - BE}{AD - BC} \\ S_{21} &= \frac{DG - CH}{AD - BC} \;;\; S_{22} = \frac{AH - BG}{AD - BC} \end{aligned} \tag{5}$$

where:

$$\begin{aligned} A &= R_{121}S_{211} + R_{122} + R_{123}S_{221} \\ B &= R_{121}S_{212} + R_{124} + R_{123}S_{222} \\ C &= R_{141}S_{211} + R_{142} + R_{143}S_{221} \\ D &= R_{141}S_{212} + R_{144} + R_{143}S_{222} \\ E &= R_{111}S_{211} + R_{112} + R_{113}S_{221} \\ F &= R_{111}S_{212} + R_{114} + R_{113}S_{222} \\ G &= R_{131}S_{211} + R_{132} + R_{133}S_{221} \\ H &= R_{131}S_{212} + R_{134} + R_{133}S_{222} \end{aligned} \tag{6}$$

$$\begin{aligned} R_{111} &= \frac{S_{124}}{S_{124}S_{113} - S_{114}S_{123}} \;;\; R_{121} = \frac{S_{133}S_{124} - S_{134}S_{123}}{S_{124}S_{113} - S_{114}S_{123}} \\ R_{131} &= \frac{S_{123}}{S_{114}S_{123} - S_{113}S_{124}} \;;\; R_{141} = \frac{S_{144}S_{123} - S_{143}S_{124}}{S_{114}S_{123} - S_{113}S_{124}} \\ R_{112} &= \frac{S_{111}S_{124} - S_{121}S_{114}}{S_{123}S_{114} - S_{113}S_{124}} \;;\; R_{132} = \frac{S_{111}S_{123} - S_{113}S_{121}}{S_{113}S_{124} - S_{114}S_{123}} \\ R_{122} &= \frac{S_{131}S_{124} - S_{121}S_{134} + R_{112}\left(S_{133}S_{124} - S_{123}S_{134}\right)}{S_{124}} \\ R_{142} &= \frac{S_{141}S_{123} - S_{143}S_{121} + R_{132}\left(S_{144}S_{123} - S_{143}S_{124}\right)}{S_{123}} \\ R_{113} &= \frac{S_{114}}{S_{123}S_{114} - S_{124}S_{113}} \;;\; R_{123} = \frac{S_{133}S_{114} - S_{134}S_{113}}{S_{123}S_{114} - S_{124}S_{113}} \\ R_{133} &= \frac{S_{113}}{S_{124}S_{113} - S_{123}S_{114}} \;;\; R_{143} = \frac{S_{144}S_{113} - S_{143}S_{114}}{S_{124}S_{113} - S_{123}S_{114}} \\ R_{114} &= \frac{S_{112}S_{124} - S_{122}S_{114}}{S_{123}S_{114} - S_{113}S_{124}} \;;\; R_{134} = \frac{S_{112}S_{123} - S_{113}S_{122}}{S_{113}S_{124} - S_{114}S_{123}} \\ R_{124} &= \frac{S_{132}S_{124} - S_{122}S_{134} + R_{114}\left(S_{133}S_{124} - S_{123}S_{134}\right)}{S_{124}} \\ R_{144} &= \frac{S_{142}S_{123} - S_{143}S_{122} + R_{134}\left(S_{144}S_{123} - S_{143}S_{124}\right)}{S_{123}} \end{aligned} \tag{7}$$

The more isolated are the LISN ports between them (S_{114}, S_{141}, S_{123}, S_{132}, S_{112}, S_{121}, S_{134}, S_{143} tending to be zero), more accurate the results of the deembedding technique will be.

V. EXPERIMENTAL VALIDATION

To validate both proposed measurement methods (interpolation and deembedding), a real equipment has been measured: a 200 W switching power supply.

V.1 Interpolation

Fig. 5 shows the measurement for the S_{11} parameter employing the method described in [4] [5], and the interpolation method presented in this paper. The peaks observed in previous methods show the inaccuracy of the S-parameter measurement, because of the fact that the interferences generated by the EUT at those frequencies are high enough to disturb the wave produced by the network analyzer. The interpolation method corrects those measurement errors eliminating the peaks.

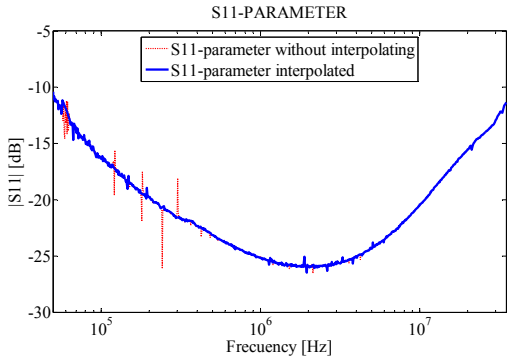

Fig. 5. S_{11} parameter comparison with and without interpolation.

V.2 Deembeding

Fig. 6 shows the S_{12} parameter measurement employing the calibration method on the LISN ports described in [4] and [5], and the calibration method on the network analyzer ports with the subsequent application of the deembedding technique presented in this paper. It can be observed that both methods have similar results, corroborating the validity of the presented method. The deembedding technique will allow the use of any network analyzer without the calibration limitation imposed by the previous methods.

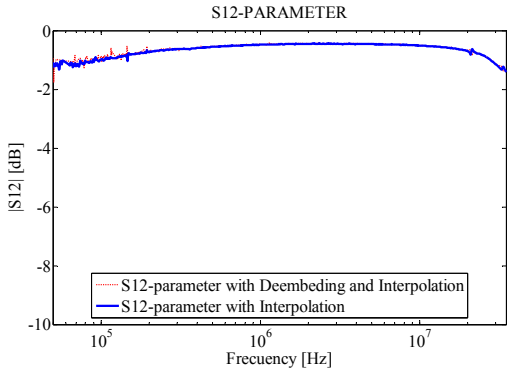

Fig. 6. S_{12} parameter comparison with and without deembedding.

VI. CONCLUSIONS

This paper presents and validates two new methods that improve the S-parameter measurement of electronic equipment connected to the power line. They allow a better characterization of the input impedance of a EUT by means of its equivalent circuital and modal models based in a three impedance pi-network. Both methods, interpolation and deembedding, can be used together or independently, to get a correct measurement.

The methods have been tested with real equipment, and it has been proved that they improve the results in front of the ones obtained with the previous measurement methods.

VII. AKNOWLEDGEMENT

This work has been financed by the TEC2004-02196 and TEC2005-04238 projects given by the *Ministerio de Educación y Ciencia* of the Spanish Government.

REFERENCES

[1] ANSI C63.13, *American National Standard Guide on the Application and Evaluation of EMI Power-Line Filters for Commercial Use*, American National Standards Institute, June 28, 1991

[2] CISPR 17, *Methods of measurement of the suppression characteristics of passive radio interference filters and suppression components*, International Electrotechnical Commission, 1981

[3] J.R. Regué, M. Ribó, D. Duran, D. Badia and A. Pérez, *Common and Differential Mode Characterization of EMI Power-Line Filters from S-parameters Measurements*, Proc. of IEEE International Symposium on EMC, August 9-13, 2004, Santa Clara, CA, pp. 610-615 vol.2

[4] J.R. Regué, M. Ribó, D. Duran, D. Badia and A. Pérez, *Measurement and modeling of noise source impedance of electronic equipment*, Proc. of the 6th EMC Europe International Symposium, September 6-10, 2004, Eindhoven, The Netherlands, pp. 150-154

[5] A. Pérez, J.R. Regué, M. Ribó, A.M. Sánchez, F.J. Pajares, D. Badia, *Circuital Characterization of an Electronic Equipment for Narrow-Band Conducted Emissions*, Proc. of the 7th EMC Europe International Symposium, September 5-8, 2006, Barcelona, Spain, pp. 1035-1040

[6] D.M. Pozar, *Microwave Engineering*, John Wiley & Sons, Inc., USA, 1998

[7] R. Bauer and P. Penfield, *De-embedding and Unterminating*, IEEE Transactions on MTT, March, 1974, vol. MTT-22, pp. 282-288.

[8] *Scorpion Embedding/De-embedding Application Note /GIP*, 11410-00278, May, 2002, http://www.us.anritsu.com/downloads/files/11410-00278B.pdf

Circuital Characterization of an Electronic Equipment for Narrow-Band Conducted Emissions

A. Pérez, J.R. Regué, M. Ribó, A.M. Sánchez, F.J. Pajares, D. Badia
antonip@salleurl.edu, jramon@salleurl.edu, mrp@salleurl.edu, albertm@salleurl.edu, fpajares@salleurl.edu, david@salleurl.edu
Department of Communications and Signal Theory
Enginyeria i Arquitectura La Salle (Ramon Llull University)
Passeig Bonanova 8, 08022 Barcelona, Spain

Abstract: In this paper, a new network analyzer-based procedure is presented in order to find the equivalent circuit for conducted interference generation of an electronic equipment when it is connected to the power line. The equivalent circuit is composed by three impedances and two voltage sources, which model the conducted interference that the electronic device injects to the power line. An accurate model of the interference generation process is very necessary in order to design or choose a suitable power line filter, or to predict the levels of conducted EMI as a function of the impedance presented by the power line. The new procedure is experimentally tested using real measurements.

I. INTRODUCTION

In order to design or choose an efficient power line filter it is necessary to fully characterize the interference generation behavior of the electronic device to which it will be connected in order to be able to predict the actual attenuation of the filter, and the levels of interference that the filtered device will supply to the power line as conducted emissions.

In [1], a complete characterization of a power line filter is presented. It is characterized by its S-parameters, both physical and modal. This characterization is more general than those based only on measuring separately common and differential mode attenuations [2] since it takes into account spurious interference flows among ports due to unbalances in the design of the filter. It can therefore account for spurious mode conversions in the filter, from common to differential mode and vice versa. In order for this characterization to be useful in a design context, a similar characterization, either considering the physical ports of the electronic device (line-ground and neutral-ground) or its equivalent modal (common and differential) ones, has to be used.

In [3], a complete model (both using physical and modal ports) for the electronic device impedance behavior (as seen from its power line cable) is presented. The electronic device is modeled by a three-impedance pi-network equivalent circuit, which is obtained from S-parameter measurements, considering the electronic device as a two port device: line-ground and neutral-ground. From this model, an equivalent modal model can then be obtained. With this model, the actual attenuation of a power line filter connected to the electronic device can be predicted. But, since it lacks information about the interference sources, it can not be used to predict the interference level generated by the electronic device after the power line filter.

In this paper, a complete circuit model for the conducted interference generation behavior of an EUT (equipment under test) is presented and tested. It extends the results of [3] (providing some modifications to be described below). A new measurement technique, also based on the utilization of a network analyzer and a LISN, is proposed in order to obtain a more complete equivalent circuit, composed by three impedances in a pi-network configuration and two voltage sources, which model the narrowband interference generated by the electronic device. The procedure is valid for frequencies in the typical working frequency ranges of the LISN. Since this model contains voltage sources that accurately model the interference sources, it can be used to predict the behavior of the interference levels when the EUT is connected to any load (power line filter, power line, etc).

II. EQUIVALENT CIRCUIT MODEL

From the point of view of a conducted EMI, the three power line terminals of a EUT (Fig. 1) can be analyzed as a two-port network (Fig. 2). Port "L" is defined between the line terminal and ground terminal. Port "N" is defined between the neutral and the ground terminals.

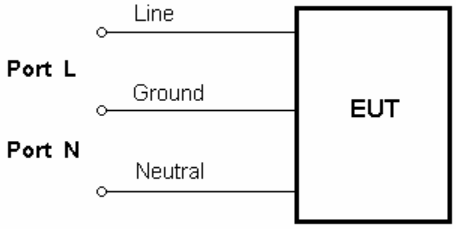

Fig. 1. Port definition for the EUT.

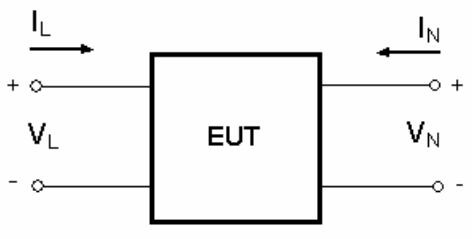

Fig. 2. Two-port equivalent circuit for the EUT.

The EUT of Fig. 2 can be modeled by a three impedance pi-network plus two external sources of interferences series-connected to the "L" and "N" terminals (Fig. 3) [4]. These equivalent AC sources generate the same interference at the terminals as the internal interference sources of the EUT.

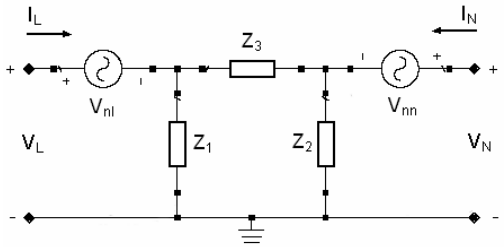

Fig. 3. Circuit model for the EUT.

II.1 Three-impedance pi-network

The three impedances (Z_1, Z_2 and Z_3) of the circuit model of Fig. 3 can be found from S-parameter measurements at both ports of the EUT:

$$Z_1 = \frac{Z_o\left(1+S_{11}\right)\left(1+S_{22}\right)-Z_oS_{12}S_{21}}{\left(1-S_{11}\right)\left(1+S_{22}\right)+S_{12}S_{21}-2S_{21}}$$
$$Z_2 = \frac{Z_o\left(1+S_{11}\right)\left(1+S_{22}\right)-Z_oS_{12}S_{21}}{\left(1+S_{11}\right)\left(1-S_{22}\right)+S_{12}S_{21}-2S_{21}} \quad (1)$$
$$Z_3 = \frac{Z_o\left(1+S_{11}\right)\left(1+S_{22}\right)-Z_oS_{12}S_{21}}{2S_{21}}$$

where Z_o is the reference impedance of the measurement system, port 1 is the "L" port and port 2 is the "N" port.

In [3], the measured S-parameters where converted to ABCD parameters, and from these, the values of the three impedances where extracted. In this paper the impedances are found directly from the measured S-parameters, obtaining a better conditioned system that reduces the error propagation.

In the S-parameter measurement process the following remarks must be taken into account:

- The EUT must continue to operate properly once the network analyzer has injected to it the adequate power to perform the measurement.
- In order to obtain a correct measurement, the power of the interference generated by the EUT must be negligible as compared with the RF power supplied by the network analyzer.

II.2 Interference sources

The values of the two external voltage sources of interference (V_{nl}, V_{nn}) present in the circuit model of Fig. 3 are found from the measurement (the measurement system is described below) of voltages and currents at the terminals of the EUT: V_L, I_L, V_N and I_N. The relationships between these parameters are:

$$I_L = \frac{V_L - V_{nl}}{Z_1} + \frac{V_L - V_{nl} - V_N + V_{nn}}{Z_3}$$
$$I_N = \frac{V_N - V_{nn}}{Z_2} + \frac{V_N - V_{nn} - V_L + V_{nl}}{Z_3} \quad (2)$$

From these equations, the two external voltage sources of interference (V_{nl}, V_{nn}) can be isolated:

$$V_{nl} = V_L - \frac{Z_1\left(Z_2+Z_3\right)I_L + Z_1Z_2I_N}{Z_1+Z_2+Z_3}$$
$$V_{nn} = V_N - \frac{Z_2\left(Z_1+Z_3\right)I_N + Z_1Z_2I_L}{Z_1+Z_2+Z_3} \quad (3)$$

III. MEASUREMENT SYSTEM

Two kinds of measurements are needed in order to find the circuit model (Fig. 3) of an EUT:

- Measurement of the S-parameters at the ports "L" and "N" of the EUT (Fig. 1), from which the values of the impedances Z_1, Z_2, Z_3 are found (see subsection II.1). The measurement system, based on a network analyzer and a LISN, is described in [3].
- Measurement of the voltages and the currents at the ports "L" and "N" of the EUT (V_L, I_L, V_N, I_N) (Fig. 3), from which the voltages of the interference voltage sources V_{nl} and V_{nn} are found (equation (3)). In this paper a new measurement system for these interference voltage sources is presented that takes advantage of the instrumentation described in [3].

The set-up used to measure the voltages and currents at the terminals of the EUT (Fig. 4) consists of a network

analyzer and a coupling network (LISN). The coupling network couples the network analyzer RF ports to the "L" and "N" ports of the EUT and protects the network analyzer from the 50 Hz high voltage of the power line. So, the LISN is used as in conducted emission tests.

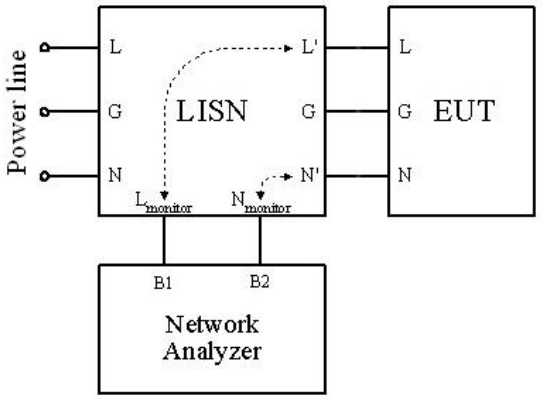

Fig. 4. Block diagram of the measurement system.

The LISN power supply connectors are connected to the EUT as in a conducted emission test, whereas line and neutral monitor connectors are connected to both ports of the network analyzer. A network analyzer is needed to perform the measurement because the amplitude of the voltages present at the EUT port must be simultaneously measured in to be able to recover the relative phase between them.

The set composed by the EUT, the network analyzer, the LISN and the cables can be represented as in Fig. 5. The network analyzer measures the values of the voltages V_{BL} (amplitude and reference (null) phase) and V_{BN} (amplitude and phase relative to V_{BL}). Therefore it is necessary to compensate the effects of the LISN and the cables, in order to obtain the voltages V_L and V_N, since these voltages are the ones which allow the computation of the interference source voltages V_{nl} and V_{nn} (equation (3)), and not the measured voltages V_{BL} and V_{BN}. In order to find V_L and V_N:

1. The S-parameters of the set composed of the LISN and the interconnection cables are measured (S_L and S_N).
2. The S-parameters S_L and S_N are transformed into the Z-parameters Z_L and Z_N using the following expressions [5]:

$$
\begin{aligned}
Z_{11} &= \frac{Z_o\left(1+S_{11}\right)\left(1-S_{22}\right)+Z_oS_{12}S_{21}}{\left(1-S_{11}\right)\left(1-S_{22}\right)-S_{12}S_{21}} \\
Z_{12} &= \frac{2Z_oS_{12}}{\left(1-S_{11}\right)\left(1-S_{22}\right)-S_{12}S_{21}} \\
Z_{21} &= \frac{2Z_oS_{21}}{\left(1-S_{11}\right)\left(1-S_{22}\right)-S_{12}S_{21}} \\
Z_{22} &= \frac{Z_o\left(1-S_{11}\right)\left(1+S_{22}\right)+Z_oS_{12}S_{21}}{\left(1-S_{11}\right)\left(1-S_{22}\right)-S_{12}S_{21}}
\end{aligned}
\tag{4}
$$

3. The voltages V_{BL} and V_{BN} are measured (both their amplitudes and relative phase).
4. The voltages V_L and V_N, and the currents I_L and I_N, are found using the following equations:

$$
\begin{aligned}
V_L &= Z_{21L}I_{BL} - Z_{22L}I_L \\
V_N &= Z_{21N}I_{BN} - Z_{22N}I_N \\
I_L &= \frac{Z_{11L}I_{BL} - V_{BL}}{Z_{12L}} \\
I_N &= \frac{Z_{11N}I_{BN} - V_{BN}}{Z_{12N}}
\end{aligned}
\tag{5}
$$

$$
\begin{aligned}
I_{BL} &= -\frac{V_{BL}}{Z_o} \\
I_{BN} &= -\frac{V_{BN}}{Z_o}
\end{aligned}
\tag{6}
$$

where Z_o is the reference impedance of the measurement system (50 Ω in our case). Substituting equation (6) in equation (5) the voltages and currents for the EUT terminals are obtained:

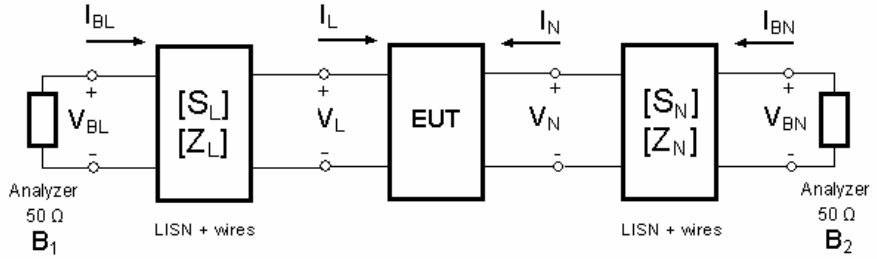

Fig. 5. Equivalent circuit of the measurement system.

$$
\begin{aligned}
V_L &= V_{BL}\left(\frac{Z_{22L}}{Z_{12L}}+\frac{Z_{11L}Z_{22L}}{Z_o Z_{12L}}-\frac{Z_{21L}}{Z_o}\right)\\
V_N &= V_{BN}\left(\frac{Z_{22N}}{Z_{12N}}+\frac{Z_{11N}Z_{22N}}{Z_o Z_{12N}}-\frac{Z_{21N}}{Z_o}\right)\\
I_L &= -V_{BL}\left(\frac{Z_{11L}}{Z_o Z_{12L}}+\frac{1}{Z_{12L}}\right)\\
I_N &= -V_{BN}\left(\frac{Z_{11N}}{Z_o Z_{12N}}+\frac{1}{Z_{12N}}\right)
\end{aligned}
\qquad (7)
$$

5. Finally, using equation (3), the interference equivalent sources V_{nl} and V_{nn} are computed.

The measurement frequency range is limited by the coupling network used. The minimum frequency depends on impedance of the inductor of the LISN. In order to reduce this frequency, a LISN with a larger inductance should be used. The maximum frequency depends on the tolerances of the other LISN components. However, for the frequency margins involved in conducted emissions, this is not a real limitation.

IV. EXPERIMENTAL VALIDATION AND RESULTS

IV.1 Experimental validation

In order to validate the proposed model and measurement procedure, the test circuit of Fig. 6 has been implemented and measured.

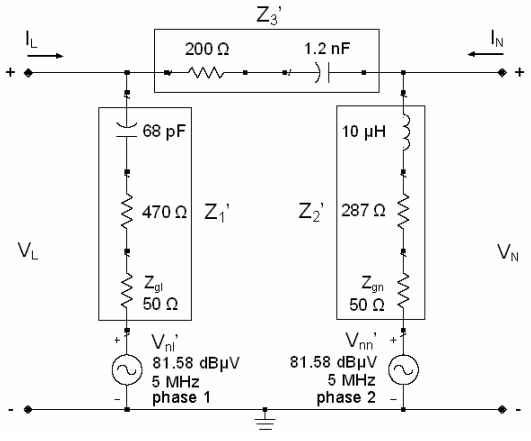

Fig. 6. Test circuit for experimental validation of the proposed procedure.

The circuit of Fig. 6 has been implemented instead of one with a structure like that of the circuit of Fig. 3 because in the circuit of Fig. 6 the two generators have a common reference and are easier to implement using laboratory instrumentation. The interference sources V_{nl}' and V_{nn}' have been generated using an RF generator and a power divider with two outputs with equal amplitude and a phase difference of 180º.

Theoretical values of the circuit model (Fig. 3) for the test circuit of Fig. 6 can be obtained using next equation:

$$
\begin{aligned}
Z_1 &= Z_1'\\
Z_2 &= Z_2'\\
Z_3 &= Z_3'\\
V_{nl} &= \frac{(Z_2+Z_3)V_{nl}'+Z_1V_{nn}'}{Z_1+Z_2+Z_3}\\
V_{nn} &= \frac{(Z_1+Z_3)V_{nn}'+Z_2V_{nl}'}{Z_1+Z_2+Z_3}
\end{aligned}
\qquad (8)
$$

Table I shows the value of the three impedances (Z_1', Z_2' and Z_3') of the test circuit of Fig. 6, which are equal to the three impedances (Z_1, Z_2 and Z_3) of the circuit model of Fig. 3, obtained in two different ways:

- Column 1: measured values of individual impedances (measured one by one with the network analyzer).
- Column 2: computed values of impedances from S-parameter measurements (subsection II.1) using the set-up described in [3].

Table I. Pi-network impedance measurements.

	Measured individual Z [Ω]	*Computed Z from measured S-param. [Ω]*
Z_1	525 - j474	489 - j486
Z_2	335 + j310	350 + j314
Z_3	203 - j24	201 - j26

Table II lists the amplitudes and phases of the interference sources of the circuit model (Fig. 3) for the test circuit of Fig. 6, both the theoretical ones (using equation (8)) and the measured ones (using the procedure described in section III and using the set-up of Fig. 4). As can be seen, the amplitudes of the interference sources inferred from the measurements agree with the theoretical ones (within 1 dB of error), as does the phase difference, which is 26.91º for the theoretical sources, and 27.95º for the inferred sources. Therefore there is a good agreement between the theoretical values of the circuit and the ones computed from the measurements made. This fact validates the measurement method proposed above for obtaining the equivalent circuit model of the EUT.

Table II. Interference source measurements.

	Theoretical sources level[dBμV]; phase [º]	*Measured sources level[dBμV] ; fase[º]*
V_{nl}	78.53 ; 0	77.43 ; 0
V_{nn}	79.98 ; 26.91	79.05 ; 27.95

Table III. Circuit model parameters at 602.17 KHz.

Z_1	486 – j2014 Ω
Z_2	2654 – j1679 Ω
Z_3	6.2 – j1.4 Ω
V_{nl}	59.82 dBμV ; 183 º
V_{nn}	65.01 dBμV ; 166 º

IV.2. Circuit model for a switched power supply

As an example of an actual circuit model for a commercial EUT, the circuit model for a personal computer switched power supply of 200 W is obtained. First of all, a conducted emission test according to regulation CISPR 22 is performed on both ports of the device (ports "L" and "N"), in order to identify the main interfering frequencies generated by the device in the range from 150 kHz to 30 MHz (Fig. 7). It can be verified that the conducted emissions are very similar in both ports, and that the interferences are narrowband.

Then, for each of the interferences with levels greater than or close to the limits established by the regulation, the equivalent circuit of Fig. 3 can be obtained. As an example of results, Table III lists the circuit parameters of the model of Fig. 3 for an interference at 602.17 KHz.

V. CONCLUSIONS

In this paper, a complete model for an EUT as a conducted interference generator is presented and tested. The model, which is the most generic model possible, takes into account all possible effects present at the EUT. A procedure for the measurement of the parameters of the model is also described. This procedure computes the model parameters from measurements made in a configuration similar to the one used in a conducted emission test, but using a network analyzer instead of an EMI receiver.

The circuit model presented in this paper can also be used to characterize the behavior of the power line as far as impedance and interference is concerned. In order to do this, a few minor changes in the described measurement method have to be done.

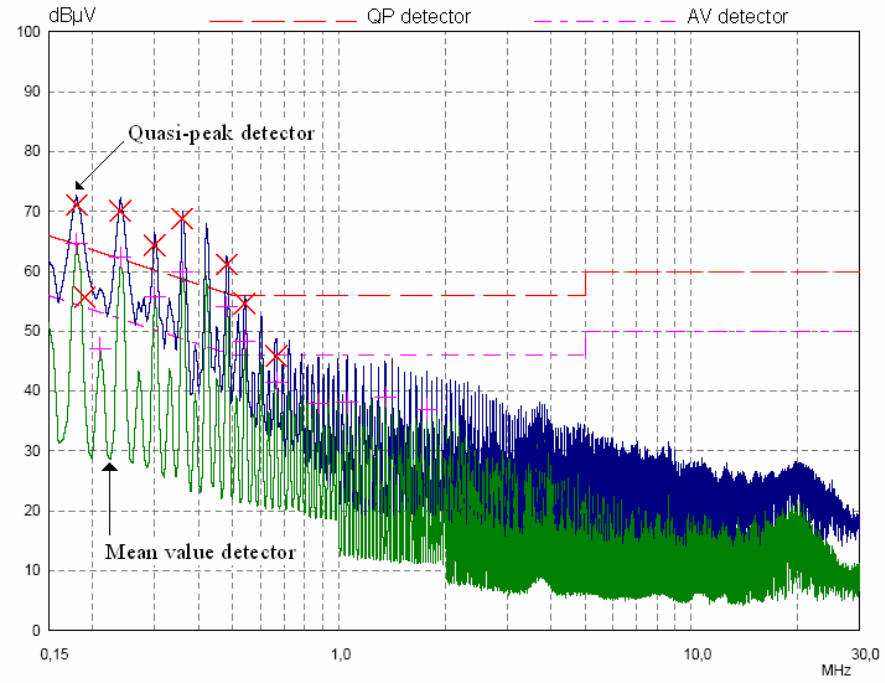

Fig. 7. Conducted emission measurement at the "L" port.

The new model and measurement procedure has been tested using a known test circuit, predicting accurately its parameters. Finally, it has been applied to the characterization of the behavior, as an interference source, of a switched power supply.

VI. AKNOWLEDGEMENT

This work has been funded by the projects TEC2004-02196 and TEC2005-04238 from the Spanish Ministerio de Educación y Ciencia.

REFERENCES

[1] J.R. Regué, M. Ribó, D. Duran, D. Badia and A. Pérez, *Common and Differential Mode Characterization of EMI Power-Line Filters from S-parameters Measurements*, Proc. of IEEE International Symposium on EMC, August 9-13, 2004, Santa Clara, CA, pp. 610-615 vol.2

[2] ANSI C63.13, *American National Standard Guide on the Application and Evaluation of EMI Power-Line Filters for Commercial Use*, American National Standards Institute, June 28, 1991

[3] J.R. Regué, M. Ribó, D. Duran, D. Badia and A. Pérez, *Measurement and modeling of noise source impedance of electronic equipment*, Proc. of the 6th EMC Europe International Symposium, September 6-10, 2004, Eindhoven, The Netherlands, pp. 150-154

[4] Guillermo González, *Microwave Transistor Amplifiers (2nd edition)*, Prentice-Hall, Inc., USA, 1997.

[5] D.M. Pozar, *Microwave Engineering*, John Wiley & Sons, Inc., USA, 1998.

Common and Differential Mode Characterization of EMI Power-Line Filters from S-parameters Measurements

Joan-Ramon Regué, Miquel Ribó, Daniel Duran, David Badia, Antonio Pérez
Department of Communications and Signal Theory
Enginyeria La Salle – Universitat Ramon Llull
Barcelona, Catalonia, Spain
jramon@salleURL.edu, mrp@salleURL.edu, danid@salleURL.edu, david@salleURL.edu, antonip@salleURL.edu

***Abstract*—In this paper a new technique to predict the small signal behavior of EMI power-line filters is presented. This technique is based on S-parameter measurements performed at all the terminals of the power-line filter. These measured S-parameters are converted to a set of modal S-parameters using the analytical matrix expressions presented in this paper. The modal S-parameter matrix completely models the small signal behavior of the power-line filter in terms of line and load common and differential modes. From this matrix, information such as common and differential mode insertion loss, modal behavior of the filter at different line and load impedances, and energy transfer between any combination of modes can be obtained.**

Keywords: EMI power-line filter, common mode, differential mode, S-parameters, measurements.

I. INTRODUCTION

The methods usually used to characterize EMI power-line filters are specified by standards [1] and [2]. They are based on filter insertion loss measurements, both in common and differential mode, with 50 ohm source and load impedances. These methods are not useful to predict the behavior of the filter in a real environment, with source and load impedances different from 50 ohm.

S-parameters completely characterize the behavior of an RF network, and can be used to characterize EMI power-line filters [3]. In this paper a new method to characterize the common mode and differential mode behavior from S-parameters measurements in the filter terminals is presented. This method is useful to predict the energy transfer between any combination of input and output modes, as well as to analyze the behavior of the filter in different source and load impedances conditions.

II. DETERMINATION OF THE MODAL S-PARAMETER MATRIX

Let us suppose we have S-parameters [4] measurements of a two-pole EMI filter, as shown in fig. 1(a). This two pole filter has four ports; each of these ports is referenced to the ground terminal of the filter. The measured S-parameter matrix relates

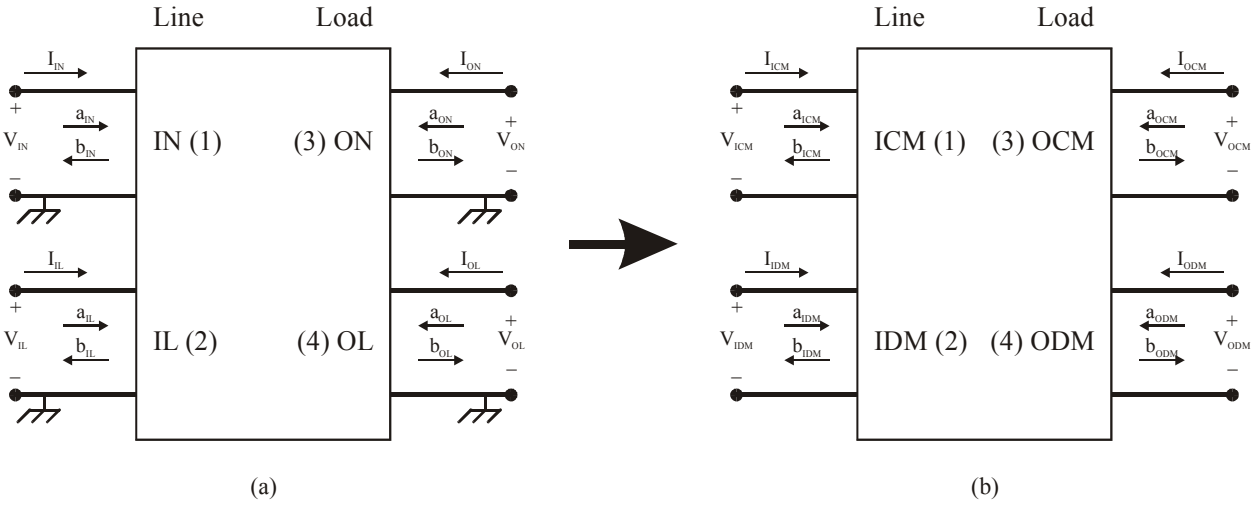

Figure 1. Port definition of S-parameters: measured (a) and modal (b).

the outgoing b waves with the incoming a waves of each port of the filter.

$$[b]=[S]\cdot[a] \tag{1}$$

$$[b]=\begin{bmatrix} b_{IN} \\ b_{IL} \\ b_{ON} \\ b_{OL} \end{bmatrix} \quad [a]=\begin{bmatrix} a_{IN} \\ a_{IL} \\ a_{ON} \\ a_{OL} \end{bmatrix} \tag{2}$$

As we are interested in the common and differential mode behavior of the EMI filter, we need to know a new S-parameter matrix relating the input common and differential modes with the output common and differential modes (fig. 1(b)). This matrix, called S_M, relates the outgoing waves b_M with the incoming a_M waves of each mode.

$$[b_M]=[S_M]\cdot[a_M] \tag{3}$$

$$[b_M]=\begin{bmatrix} b_{ICM} \\ b_{IDM} \\ b_{OCM} \\ b_{ODM} \end{bmatrix} \quad [a_M]=\begin{bmatrix} a_{ICM} \\ a_{IDM} \\ a_{OCM} \\ a_{ODM} \end{bmatrix} \tag{4}$$

The main aim of this work is to derive the modal matrix S_M from the measured S.

The relation between a and b waves with voltages and currents present at each port are (5).

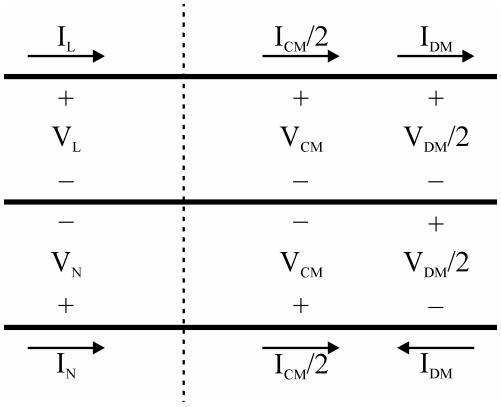

Figure 2. Relation between line and neutral, and modal voltages and currents.

$$\begin{aligned} a_L &= \frac{1}{2\sqrt{Z_0}}(V_L + Z_0 I_L) \\ a_N &= \frac{1}{2\sqrt{Z_0}}(V_N + Z_0 I_N) \\ b_L &= \frac{1}{2\sqrt{Z_0}}(V_L - Z_0 I_L) \\ b_N &= \frac{1}{2\sqrt{Z_0}}(V_N - Z_0 I_N) \end{aligned} \tag{5}$$

$$\begin{aligned} a_{CM} &= \frac{1}{2\sqrt{Z_{0CM}}}(V_{CM} + Z_{0CM} I_{CM}) \\ a_{DM} &= \frac{1}{2\sqrt{Z_{0DM}}}(V_{DM} + Z_{0DM} I_{DM}) \\ b_{CM} &= \frac{1}{2\sqrt{Z_{0CM}}}(V_{CM} - Z_{0CM} I_{CM}) \\ b_{DM} &= \frac{1}{2\sqrt{Z_{0DM}}}(V_{DM} - Z_{0DM} I_{DM}) \end{aligned} \tag{6}$$

Analyzing the relations between common and differential mode voltages and currents with line and neutral voltages and currents (fig. 2), the following relations are obtained:

$$\begin{aligned} V_L &= V_{CM} + \frac{V_{DM}}{2} \qquad I_L = \frac{I_{CM}}{2} + I_{DM} \\ V_N &= V_{CM} - \frac{V_{DM}}{2} \qquad I_N = \frac{I_{CM}}{2} - I_{DM} \end{aligned} \tag{7}$$

Substituting (7) in (5) and (6) the following equations relating modal and measured waves can be written:

$$\begin{aligned} a_{CM} &= \frac{a_L + a_N}{\sqrt{2}} \qquad b_{CM} = \frac{b_L + b_N}{\sqrt{2}} \\ a_{DM} &= \frac{a_L - a_N}{\sqrt{2}} \qquad b_{DM} = \frac{b_L - b_N}{\sqrt{2}} \end{aligned} \tag{8}$$

where:

$$\begin{aligned} Z_{0CM} &= \frac{Z_0}{2} \\ Z_{0DM} &= 2Z_0 \end{aligned} \tag{9}$$

From (8) two matrix relations between modal and measured waves are derived:

$$[a_M]=[A]\cdot[a] \tag{10}$$

$$[b_M]=[B]\cdot[b] \tag{11}$$

where:

$$[A]=[B]=\frac{1}{\sqrt{2}}\begin{bmatrix}1 & 1 & 0 & 0\\ 1 & -1 & 0 & 0\\ 0 & 0 & 1 & 1\\ 0 & 0 & -1 & 1\end{bmatrix} \quad (12)$$

Substituting (10) and (11) in (1) we obtain the relation between the modal S-parameter matrix and the measured S-parameters matrix.

$$[S_M]=[B]\cdot[S]\cdot[A]^{-1} \quad (13)$$

Using (13) we can obtain a modal S-parameter matrix, describing completely the modal behavior of the EMI filter, from an S-parameter matrix obtained with a very simple measurement configuration.

III. APPLICATIONS

As the modal S-parameter matrix obtained using (13) is a complete small signal model of power-line filters, any small signal information of filters can be deduced from it. This information from the modal S-parameter matrix can be useful to:

- Obtain equivalent information to the insertion-loss test methods specified by [1].
- Calculate the insertion-loss at different line or load impedances.
- Determine any energy transfer between any pair of line or load common or differential modes.

All the examples of the following sections are based on measurements of different power-line filters performed following the scheme of fig. 1(a). To measure these filters a network analyzer had been used to perform a conventional S-parameters four port measurement. Each of these four ports is one of the terminals of the power-line filter referenced to ground.

A. Common and differential mode insertion-loss

The first application of the method is the determination of the common and differential mode insertion-loss of a power-line filter, and particularly the determination of its insertion-loss in an equivalent way to that obtained using 50Ω insertion-loss test methods specified in power-line filter standards [1].

Analyzing measurement methods presented in [1] and comparing its definitions of common and differential mode currents and voltages to the slightly different definitions presented in this paper, it can be seen that:

$$\begin{aligned}\frac{V_{CM}}{I_{CM}}&=50\Omega\\ \frac{V_{DM}/2}{I_{DM}}&=50\Omega\end{aligned} \quad (14)$$

And therefore the characteristic impedances of each mode are:

$$\begin{aligned}Z_{0CM}&=\frac{V_{CM}}{I_{CM}}=50\Omega\\ Z_{0DM}&=\frac{V_{DM}}{I_{DM}}=100\Omega\end{aligned} \quad (15)$$

This means that it is necessary to evaluate the modal S-parameters of $[S_M]$ using the characteristic impedances of (15). Conversion from the characteristic impedances of $[S_M]$ to the new ones can be easily done by using any microwave circuit simulator. Once the new modal S-parameters matrix with the new characteristic impedances is known, common and differential mode insertion-losses are respectively S_{13} and S_{24} parameters of this new matrix.

Fig. 3 shows a comparison of common mode insertion-loss of a filter obtained using the method presented in this paper with common mode insertion-loss measured according to [1]. Fig. 4 shows the same comparison for the case of differential mode. In both cases the agreement is very good, with an error always less than 2.5dB.

The test method of [1] requires the use of a short-circuit between both line and both load terminals of the power-line filter in the case of common mode insertion-loss measurements and two splitters in the case of differential mode measurements, while the method presented in this paper connects directly the ports of a network analyzer to the terminals of the filter. Therefore the measurement method presented in this paper is simpler and has a lower measurement uncertainty than the standard method specified in [1].

B. Insertion-loss at different line and load impedances

The insertion-loss behavior of power-line filters is strongly dependent of its line and load impedances [5],[6]. Using the method presented in this paper the behavior of the filter at any line and load impedance can be calculated without any additional measurement. This job can be done evaluating, using any microwave circuit simulator, the insertion-loss of $[S_M]$ loaded with the desired line and load common and differential mode impedances.

Fig. 5 shows the common mode insertion-loss at four different common mode impedances, and fig. 6 the differential mode insertion-loss at four different differential mode load impedances. In both cases the line impedance is the equivalent impedance of a 50Ω//50μH LISN.

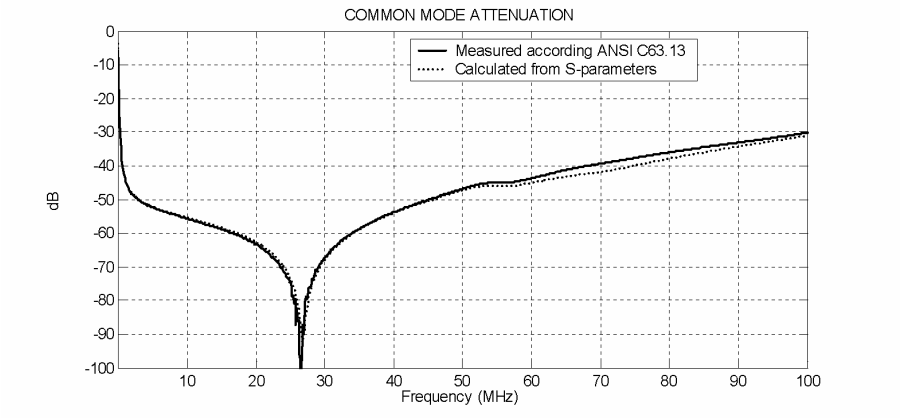

Figure 3. Common mode attenuation measured and calculated using the method.

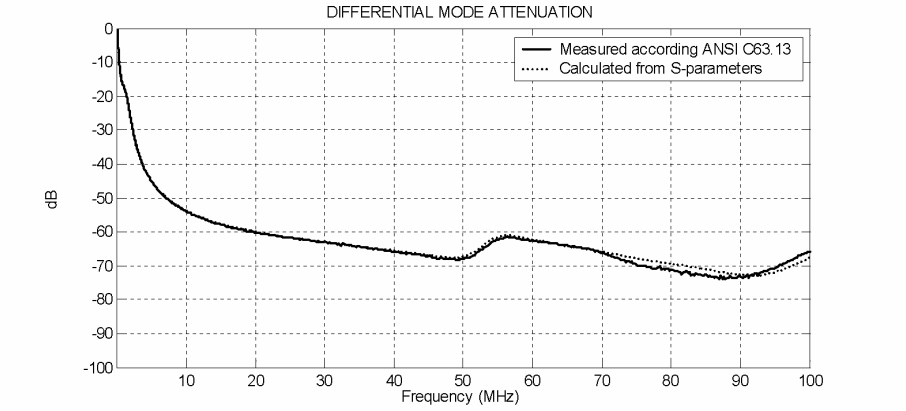

Figure 4. Differential mode attenuation measured and calculated using the method.

C. Energy conversion between common and differential modes

An additional feature of this method is its capability to determine the energy transfer between common and differential modes. The method can predict the mode conversion between line and load, and also the mode conversion in the reflected power at both sides of the filter. For instance, fig. 7 illustrates the energy transfer between load differential mode and line differential and common modes of a measured filter. It can be seen that at frequencies between 3.4 MHz and 15.4 MHz and above 20.5 MHz most of the differential power incident at the line side of the filter is transferred to the common mode at the line side of the filter. This fact demonstrates that a simple differential and common mode insertion-loss measurement is not enough to fully characterize an EMI power-line filter.

Fig. 8 shows the energy transfer between load common mode and line differential mode. In this case most of the output power is in the same input mode.

Usually power-line filters are designed to reflect all the incoming common or differential mode energy to the line or load ports. Ideally all the energy is reflected to the same exciting mode, but unidealities in the filter can cause a transfer of energy to the other mode. For instance, let us suppose that a circuit generates differential mode interference. When this interference arrives to the power-line filter is reflected in part as common mode interference. This unexpected common mode interference present at the generating circuit can cause its radiation in common mode. Fig. 9 shows the common mode reflected at the load, this reflection is mainly in common mode, but, as can be seen, a small part of this common mode energy is reflected as differential mode energy. Fig. 10 shows the reflection of the differential mode energy at the load.

IV. CONCLUSIONS

A new measurement technique, based on S-parameters, for EMI power-line filters has been presented. This technique, apart from predicting the values of insertion-loss according to conventional standards, can predict the energy transfer between any combination of common and differential modes and also predict the behavior of the filter at any line and load impedances.

The measurement setup used in the method presented in this paper is also simpler than the standard insertion-loss measurements. And as result of this the measurement uncertainty is also lower.

0-7803-8444-X/04/$20.00 (C) IEEE

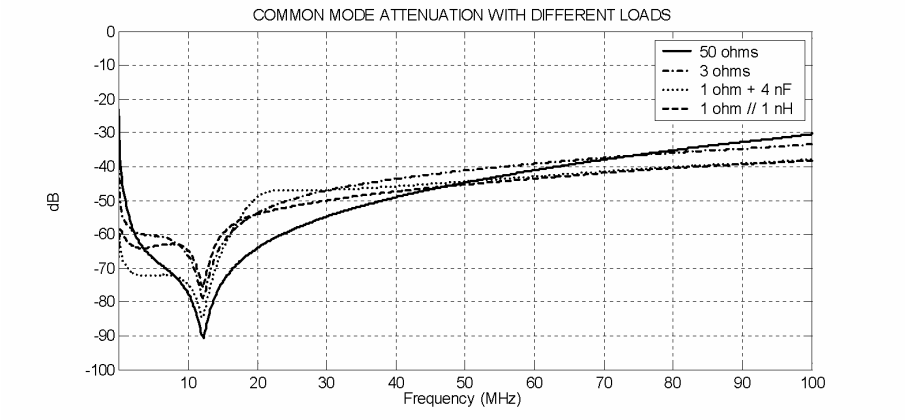

Figure 5. Common mode attenuation at different load impedances.

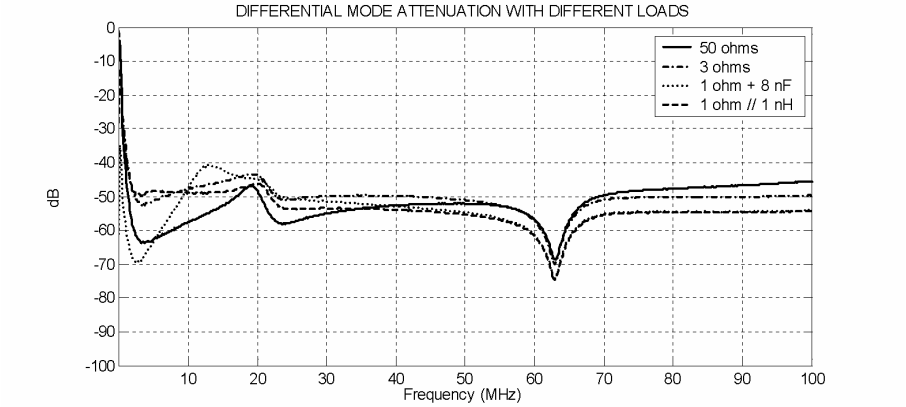

Figure 6. Differential mode attenuation at different load impedances.

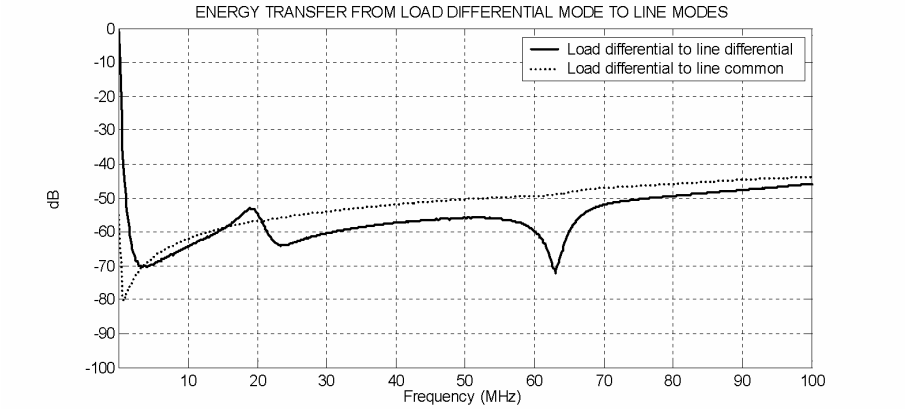

Figure 7. Energy transfer between load differential mode and line common mode.

REFERENCES

[1] ANSI C63.13, "American National Standard Guide on the Application and Evaluation of EMI Power-Line Filters for Commercial Use," *American National Standards Institute*, June 28, 1991.

[2] CISPR 17, "Methods of measurement of the suppression characteristics of passive radio interference filters and suppression components," *International Electrotechnical Commission*, 1981.

[3] J. G. Kraemer, "S-parameter Characterization for EMI filters," *in Proc. 2003 IEEE EMC Symp.*, Boston, MA, Aug. 18–22, 2003, pp. 361–366.

[4] D. M. Pozar, *Microvawe Engineering*, 2nd ed., John Wiley & Sons, 1998.

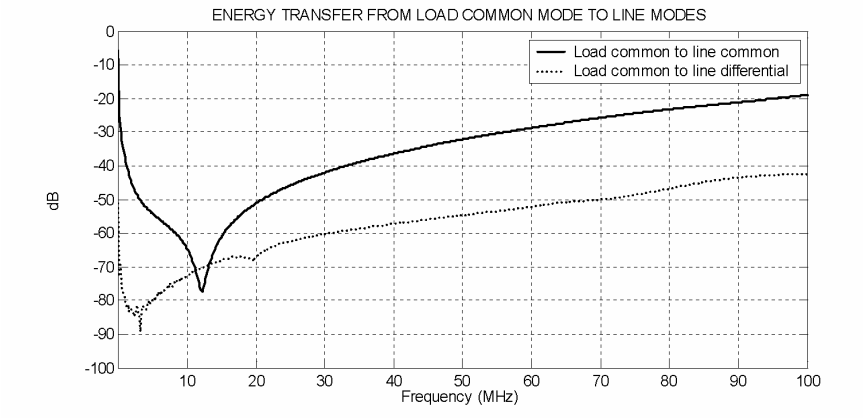

Figure 8. Energy transfer between load common mode and line differential mode.

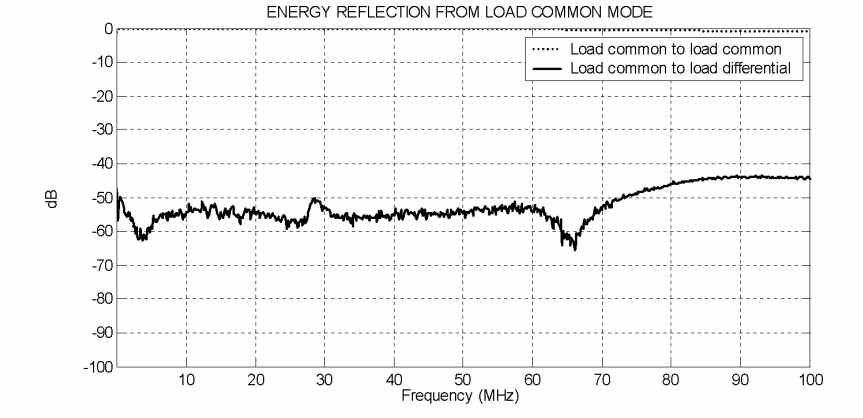

Figure 9. Energy reflection from load common mode to load differential mode.

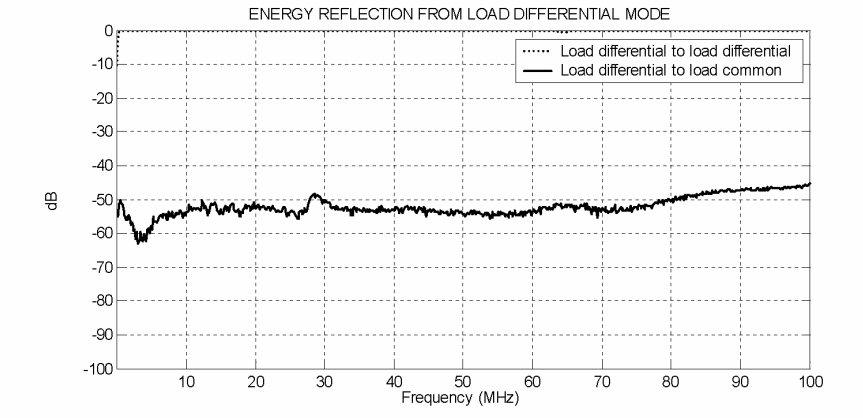

Figure 10. Energy reflection from load differential mode to load common mode.

[5] B. Garry and R. Nelson, "Effect of impedance and frequency variation on insertion loss for a typical power line filter," *in Proc. 1998 IEEE EMC Int. Symp.*, Denver, CO, Aug. 24–28, 1998, pp. 691–695.

[6] M. Kanda, N. Oka and S. Nitta, "Common mode impedance model of power electronic equipment to evaluate noise reduction effect of a line noise filter," *in Proc. 2000 IEEE EMC Int. Symp.*, Washington, DC, Aug. 21–25, 2000, pp. 65–70.

MEASUREMENT AND MODELING OF NOISE SOURCE IMPEDANCE OF ELECTRONIC EQUIPMENT

J. R. Regué, M. Ribó, D. Duran, D. Badia and A. Pérez
Department of Communications and Signal Theory, Enginyeria La Salle, Universitat Ramon Llull
Passeig Bonanova 8, 08022 Barcelona, Catalonia, Spain
E-mail: {jramon, mrp, danid, david, antonip}@salleURL.edu

Abstract: In this paper a measurement technique, based on network analyser measurements, useful to determine the noise source impedance of on-line electronic equipment is presented. Measurements performed using this technique are used to determine the values of an impedance model composed by three impedances, which is finally used to calculate the value of common and differential mode impedances and the value of the transimpedance between common and differential mode and vice versa. The knowledge of the values of these impedances can be very helpful to choose the correct EMI power-line filter or to determine the conducted emission level at any line impedance. The validity and usefulness of this technique is demonstrated by real measurements.

I. INTRODUCTION

Knowledge of noise source impedance of electronic equipment is very useful to predict the behaviour of any EMI power-line filter connected to it, and to determine its conducted emission level at different load impedances. Some techniques have been used to measure common and differential mode noise source impedances, for instance the insertion loss method [1] and the two current probes method [2].

In this paper a new model for the input impedance of electronic equipment at the power-line connector is presented. This model is valid for equipment connected to a two lines and ground power-line system, but the model is easily extensible to any three line connector. The model is based on a pi-network composed of three impedances, because it is the minimum number of impedances necessary to model a two-port network. This model can be determined by measurements performed using a LISN to couple a network analyser to the EUT. From this three impedance model, not only common and differential mode impedances are determined, but also common-to-differential and differential-to-common mode transimpedances are obtained.

II. THREE IMPEDANCE MODEL

From a RF point of view the three power-line terminals of the EUT can be analysed as a two-port network (Fig. 1(a)). Port 1 is defined between line and ground and Port 2 between neutral and ground. Assuming that this network is reciprocal, it can be fully modelled by a pi network [3] (Fig. 1(b)).

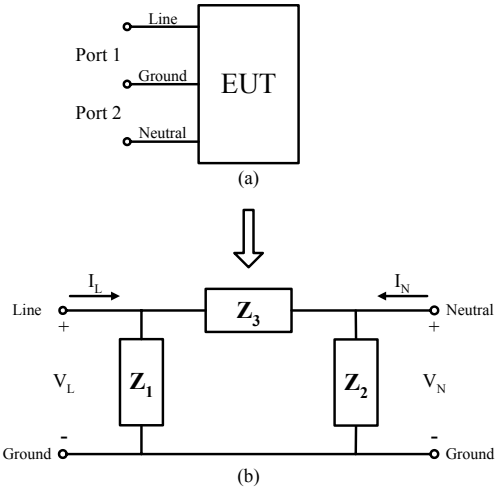

Fig. 1 - (a) Port definition of the EUT. (b) Three impedance model of the EUT.

The values of these three impedances will be found from S-parameter measurements, performed using a network analyser, of both ports of the EUT (see section IV). The measured S-parameters can be converted to its equivalent ABCD parameters [3] using

$$\begin{aligned} A &= \frac{(1+S_{11})(1-S_{22})+S_{12}S_{21}}{2S_{21}} \\ B &= Z_0\frac{(1+S_{11})(1+S_{22})-S_{12}S_{21}}{2S_{21}} \\ C &= \frac{1}{Z_0}\frac{(1-S_{11})(1-S_{22})-S_{12}S_{21}}{2S_{21}} \\ D &= \frac{(1-S_{11})(1+S_{22})+S_{12}S_{21}}{2S_{21}} \end{aligned} \qquad (1)$$

where Z_0 is the characteristic impedance of the measuring system.

Finally the values of the three impedances of the model of Fig. 1(b) can be calculated from (1) using

$$Z_1 = \frac{B}{D-1}$$
$$Z_2 = \frac{B}{A-1} \qquad (2)$$
$$Z_3 = B$$

III. CONVERSION FROM THE THREE IMPEDANCE MODEL TO THE MODAL MODEL

The three impedance model permits a complete modelling of the input impedance of an EUT, but a model in terms of common and differential mode impedances would be more interesting in order to analyse the behaviour of the EUT. The relationship between line and neutral voltages and currents can be deduced from Fig. 1(b).

$$I_L = \frac{V_L(Z_1+Z_3) - V_N Z_1}{Z_1 Z_3}$$
$$I_N = \frac{V_N(Z_2+Z_3) - V_L Z_2}{Z_2 Z_3} \qquad (3)$$

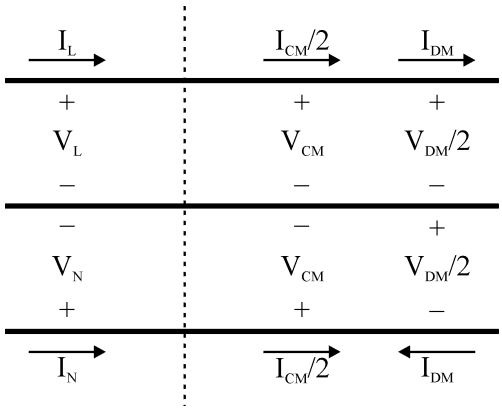

Fig. 2: Relationship between line and neutral, and modal voltages and currents.

Analysing the relationships between common mode voltage (V_{CM}), differential mode voltage (V_{DM}), common mode current (I_{CM}) and differential mode current (I_{DM}) with line and neutral voltages and currents [4] (Fig. 2), the following expressions are obtained:

$$V_L = V_{CM} + \frac{V_{DM}}{2}$$
$$V_N = V_{CM} - \frac{V_{DM}}{2} \qquad (4)$$

and

$$I_{CM} = I_L + I_N$$
$$I_{DM} = \frac{I_L - I_N}{2} \qquad (5)$$

The relationships between common and differential mode voltages and currents can be deduced operating with (3), (4) and (5).

$$I_{CM} = \frac{V_{CM}}{Z_{CM}} + \frac{V_{DM}}{Z_{DC}}$$
$$I_{DM} = \frac{V_{CM}}{Z_{CD}} + \frac{V_{DM}}{Z_{DM}} \qquad (6)$$

where Z_{CM} is the common mode impedance, Z_{DM} is the differential mode impedance, Z_{DC} is the differential mode to common mode transimpedance and Z_{CD} is the common mode to differential mode transimpedance.

As the model shown in Fig. 1 is composed only by three impedances and thanks to the definition of modal currents and voltages of Fig. 2, the transimpedances Z_{DC} and Z_{CD} are equal. Therefore both can be renamed as Z_{TM}:

$$I_{CM} = \frac{V_{CM}}{Z_{CM}} + \frac{V_{DM}}{Z_{TM}}$$
$$I_{DM} = \frac{V_{CM}}{Z_{TM}} + \frac{V_{DM}}{Z_{DM}} \qquad (7)$$

where

$$Z_{CM} = \frac{Z_1 Z_2}{Z_1 + Z_2}$$
$$Z_{DM} = \frac{4Z_1 Z_2 Z_3}{4Z_1 Z_2 + Z_1 Z_3 + Z_2 Z_3} \qquad (8)$$
$$Z_{TM} = \frac{2Z_1 Z_2}{Z_2 - Z_1}$$

The expressions in (8) can be interpreted as equivalent shunt impedances:

$$Z_{CM} = Z_1 // Z_2$$
$$Z_{DM} = Z_3 // (4Z_1) // (4Z_2) \qquad (9)$$
$$Z_{TM} = (2Z_1) // (-2Z_2)$$

In (9), Z_{CM} represents the common mode input impedance of the EUT and Z_{DM} represents the differential mode input impedance of the EUT. While Z_{TM} represents the transimpedances form differential to common and from common to differential modes.

As can be observed in (8), when the EUT is unbalanced ($Z_1 \neq Z_2$) the transimpedance Z_{TM} exists, causing a transfer of energy between modes. This corroborates the assumption that common and differential mode impedances are not enough to model the input impedance of the EUT.

IV. MEASUREMENT SYSTEM

The measurement set-up used to measure the S-parameters of the EUT (Fig. 3) is composed of a network analyser and a coupling network. The mission of the coupling network is to couple RF signals of the network analyser to the power-line input of the EUT and protect the network analyser from power-line voltages. LISNs are used in conducted emissions measurements to perform a similar task, and can also be adapted to perform S-parameter measurements.

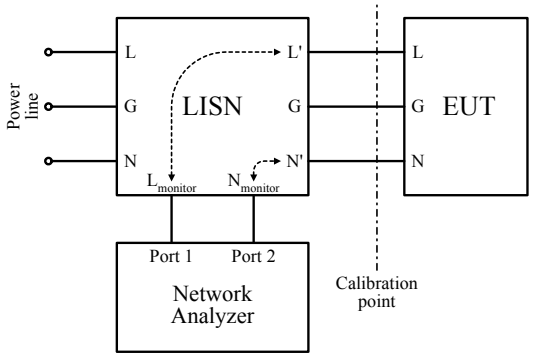

Fig. 3: Bloc diagram of the measurement system.

The Power-line connectors of the LISN are connected to the EUT as usually done in a conducted emission test, while line and neutral monitor connectors are connected simultaneously to both ports of the network analyser. In order to remove the effect of the monitor-to-EUT path, the standard calibration procedure of the network analyser is performed considering as calibration ports the EUT side of power-line terminals of the LISN.

In order to validate this calibration approach some experiments have been performed. These experiments consist in comparing measurements of different pi-networks, performed directly with the network analyser and using the set-up and calibration method of Fig. 3. Fig. 4 shows an example of these comparison, where the pi-network is composed by three standard resistors of nominal values of 11 Ω, 100 Ω and 1 kΩ, respectively. The average relative error between the impedances obtained with both methods in all the series of measurements performed was about 2.8%, corroborating the validity of the calibration approach.

The frequency range of the measurements is mainly limited by the coupling network used and by the cabling used to connect the coupling network to the EUT. In the case of Fig. 4, a 50Ω and 50μH LISN with a maximum operating frequency of 100MHz has been used. The minimum frequency depends on the impedance of the inductor of the LISN. The lower is the impedance of the inductor the higher is the calibration error in the measurement. The lower frequency range of measurements of Fig. 4 is 50kHz. A solution to extend the lower frequency range would be to use a LISN with a higher inductance.

V. EXPERIMENTAL VALIDATION

Fig. 5 shows the noise source impedance modelling of a measured operating linear DC power supply. Fig. 5(a) shows its three impedance model (Z_1, Z_2 and Z_3) and Fig. 5(b) shows its modal model (common and differential mode impedances, Z_{CC} and Z_{DD} respectively, and transimpedance Z_{TM}). As can be seen, the magnitude of transimpedance is similar to the magnitude of common mode impedance, at certain

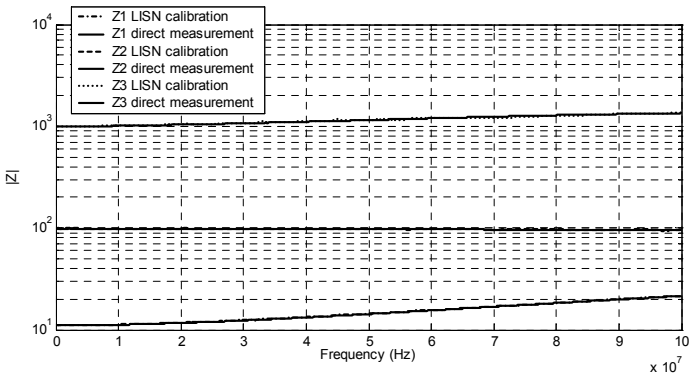

Fig. 4: Comparison between impedances obtained by direct measurement and using LISN calibration.

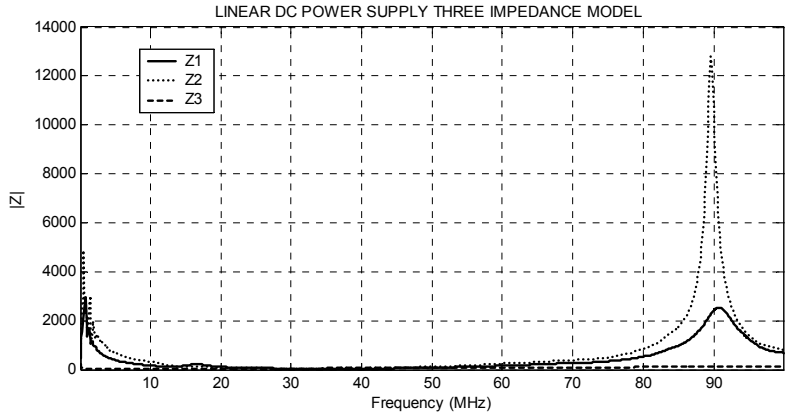

(a)

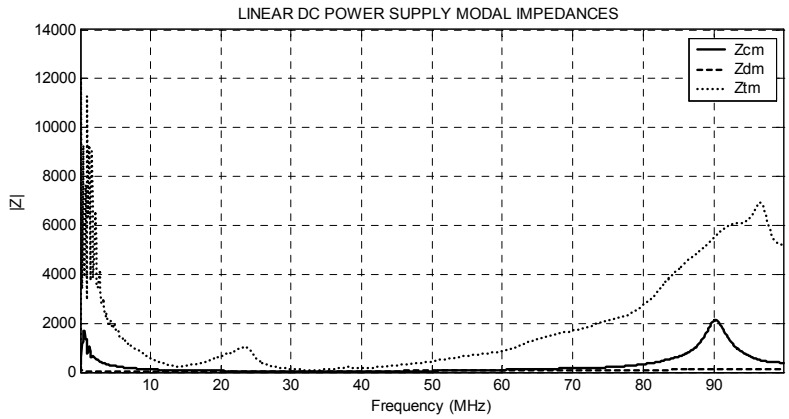

(b)

Fig. 5: Impedance measurements of an operating linear DC power supply. (a) Three impedance model. (b) Modal model.

frequencies. Therefore a high energy transfer between modes can occur at those frequencies. For instance, a common mode interference arriving from the power-line terminals at the EUT can be reflected in part as differential mode interference.

Fig. 6 is another example of measured impedances. In this case an on-line personal computer has been measured. Fig. 6(a) shows the three impedance model of the personal computer, while Fig. 6(b) shows the common and differential mode impedances and the transimpedance between modes.

VI. CONCLUSIONS

In this paper a measurement technique useful to determine the noise source impedance of EUTs has been presented. Measurements are performed using a network analyser and a LISN, and are used to determine the impedances (magnitude and phase) of a pi-network model. This three impedance model can be converted to a model which comprises common and differential mode impedances and transimpedance between modes. This transimpedance models the interchange of energy between common and differential modes, something impossible to model with the traditional models composed only of common mode and differential mode impedances. The validity and usefulness of this technique has been demonstrated by real measurements.

REFERENCES

[1] D. Zhang, D.Y. Chen, M.J. Nave, D. Sable, "Measurement of Noise Source Impedance of Off-line Converters", *Proc. of 1998 Applied Power Electronics Conference*, pp. 918-923.

[2] K.Y. See, L. Yang, "Measurement of noise source impedance of SMPS using two current probes", *IEE Electronics Letters*, vol. 36, No. 21, pp. 1774-1776, 12th Oct. 2000.

[3] D.M. Pozar, *"Microwave Engineering"*, John Wiley & Sons, Inc., USA, 1998.
[4] J.R. Regué, M. Ribó, D. Duran, D. Badia and A. Pérez, "Common and Differential Mode Characterization of EMI Power-Line Filters from S-parameters Measurements", *Proc. of 2004 IEEE Int. Symp. on EMC,* in press.

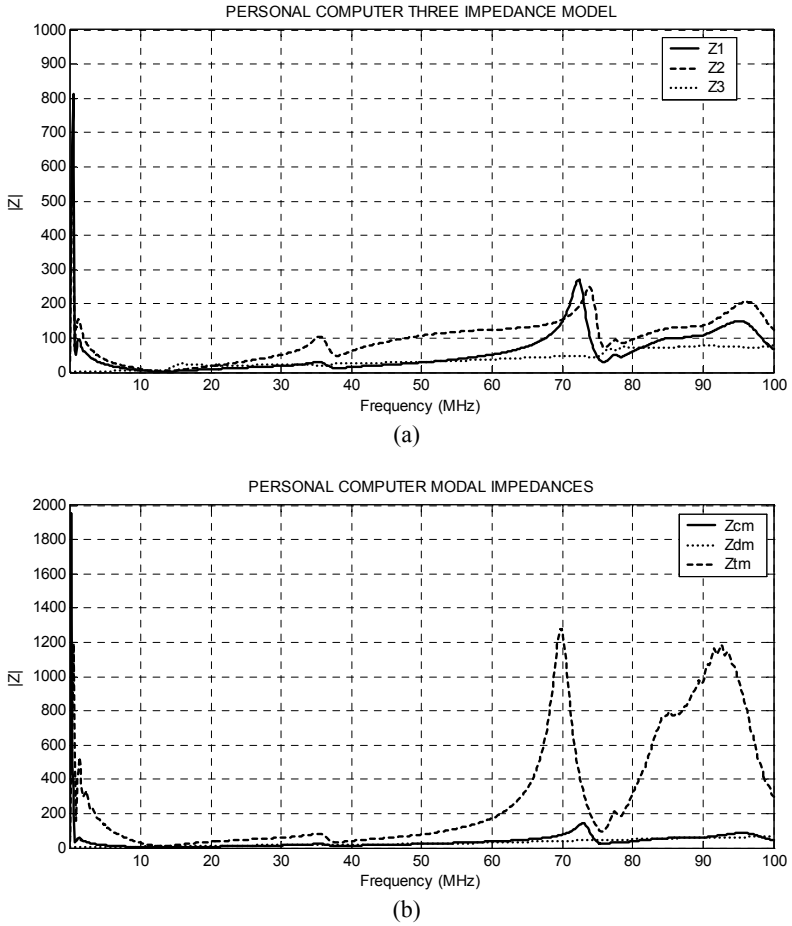

Fig. 6: Impedance measurements of an on-line personal computer. (a) Three impedance model. (b) Modal model.

Método de medida mejorado de la impedancia de entrada de equipos electrónicos

A. Pérez, A.M. Sánchez, G. Roig, J.R. Regué, M. Ribó, P. Rodríguez-Cepeda, F.J. Pajares
antonip@salle.url.edu, albertm@salle.url.edu, groig@salle.url.edu, jramon@salle.url.edu, mrp@salle.url.edu, jprodriguez@salle.url.edu, fpajares@salle.url.edu
GRECO – Grup de Recerca en Electromagnetisme i Comunicacions
Enginyeria i Arquitectura La Salle
Universitat Ramón Llull
Quatre Camins 2, 08022 Barcelona (Spain)

***Abstract* – This paper presents two new measurement methods useful to obtain a better characterization of the input impedance of electronic equipment connected to the power line. This characterization is performed using a three-impedance pi-network, which is obtained from an S-parameter measurement of the equipment. Both methods proposed in this paper improve the accuracy of S-parameter measurements, and consequently yield more accurate equivalent models. The knowledge of these models is very useful to design and/or to choice the most suitable power-line filter, since they allow the prediction of the true attenuation of the filter in common and differential modes. The new techniques are experimentally tested using real measurements.**

I. INTRODUCCIÓN

Los estándares actuales empleados para caracterizar los filtros de red [1][2] están basados en medidas de atenuación en modo común y modo diferencial con impedancias de línea y de carga de 50 Ω. Estos métodos resultan poco útiles para predecir el comportamiento del filtro en un entorno real, donde las impedancias que se presentan pueden ser muy diferentes de 50 Ω.

En [3], se caracteriza un filtro de red mediante sus parámetros S, físicos (terminales de línea y neutro) y modales (modo común y modo diferencial). Para que esta caracterización sea útil en un contexto de diseño, se ha de emplear una caracterización similar para el equipo electrónico, que considere sus puertos físicos (línea-tierra y neutro-tierra) o sus equivalentes modales (común y diferencial).

En [4][5], se presenta un modelo completo (usando puertos físicos y modales) para caracterizar la impedancia del equipo electrónico (vista desde los terminales de alimentación). El equipo se modela mediante un circuito equivalente de tres impedancias en pi, el cual se obtiene a partir de la medida de parámetros S. A partir de este modelo circuital, se obtiene un nuevo modelo modal equivalente, mediante el cual se puede predecir la atenuación real de un filtro de red conectado al equipo electrónico.

Este artículo presenta dos nuevos métodos de medida para obtener los parámetros S de un equipo electrónico conectado a la red eléctrica, que mejoran las propuestas anteriores [4][5]. Una medida de parámetros S más exacta permitirá una mejor caracterización del ESE (Equipo Sometido a Ensayo) mediante sus modelos equivalentes circuital y modal.

II. MODELO CIRCUITAL EQUIVALENTE DE UN ESE

Los tres terminales de alimentación de un ESE se pueden analizar como una red de dos puertos (Fig. 1). El puerto "L" se define entre el terminal de línea y el terminal de tierra, y el puerto "N" se define entre los terminales de neutro y tierra.

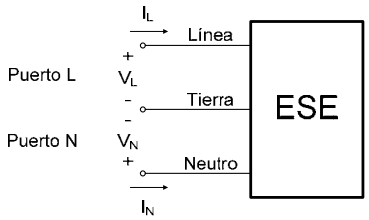

Fig. 1. Definición de puertos del ESE.

Asumiendo que esta red es recíproca, puede ser modelada mediante una red en pi [6] (Fig. 2).

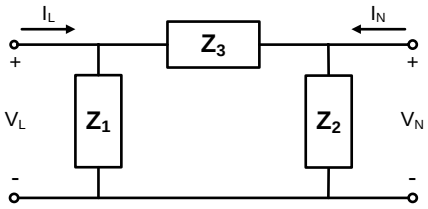

Fig. 2. Modelo circuital de tres impedancias en pi.

Las tres impedancias (Z_1, Z_2 y Z_3) del modelo circuital de la Fig. 2 se pueden hallar a partir de la medida de parámetros S en ambos puertos del ESE [5]:

$$Z_1 = \frac{Z_o\left(1+S_{11}\right)\left(1+S_{22}\right)-Z_oS_{12}S_{21}}{\left(1-S_{11}\right)\left(1+S_{22}\right)+S_{12}S_{21}-2S_{21}}$$
$$Z_2 = \frac{Z_o\left(1+S_{11}\right)\left(1+S_{22}\right)-Z_oS_{12}S_{21}}{\left(1+S_{11}\right)\left(1-S_{22}\right)+S_{12}S_{21}-2S_{21}} \quad (1)$$
$$Z_3 = \frac{Z_o\left(1+S_{11}\right)\left(1+S_{22}\right)-Z_oS_{12}S_{21}}{2S_{21}}$$

donde Z_0 es la impedancia de referencia del sistema de medida, el puerto 1 es el puerto "L" y el puerto 2 es el puerto "N".

III. LIMITACIONES DEL SISTEMA DE MEDIDA ACTUAL DE PARÁMETROS S

La configuración utilizada para medir los parámetros S del ESE (Fig. 3) consta de un analizador de redes y una red de acoplamiento (LISN: Line Impedance Stabilizing Network) [4].

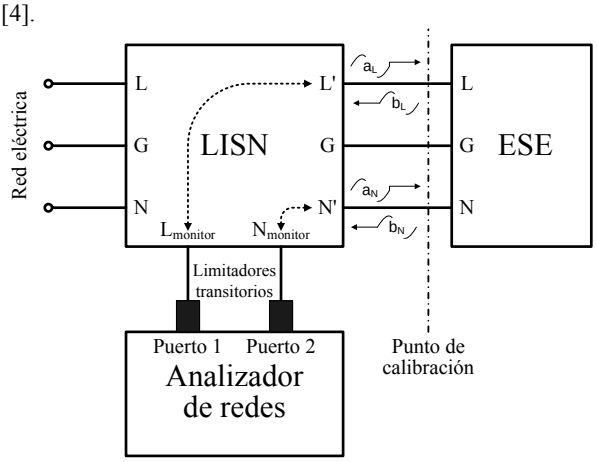

Fig. 3. Diagrama de bloques del sistema de medida.

Para compensar el efecto que provoca la LISN, los limitadores de transitorios y los cables de interconexión en la medida de los parámetros S del ESE, el proceso de calibración estándar del analizador de redes se lleva a cabo considerando como puertos de calibración los terminales de la LISN que están en contacto con el ESE.

Esta configuración de medida lleva asociadas las siguientes limitaciones:

- Para obtener una medida correcta de parámetros S, la interferencia que genera el ESE ha de ser despreciable frente a la potencia que suministra el analizador de redes. En caso contrario, la onda reflejada por el ESE puede quedar enmascarada por la propia interferencia que genera éste.
- No todos los analizadores de redes permiten una calibración como la que propone la Fig. 3; esto es compensar el efecto que producen los limitadores de transitorios, que atenúan del orden de 10 dB, conectados entre los puertos de medida (terminales de la LISN que están en contacto con el ESE) y los puertos del analizador de redes. También la LISN introduce una atenuación considerable a bajas frecuencias que hay que compensar.

El artículo propone, manteniendo el set-up inicial, dos nuevas técnicas en el proceso de medida que solucionan las limitaciones planteadas anteriormente:

- Interpolación: permite utilizar analizadores de redes que no disponen de una potencia de salida elevada, asegurando la integridad de la medida de parámetros S.
- *Deembedding*: método de cálculo para extraer los parámetros S del ESE calibrando en los puertos del analizador de redes, y no en los terminales de la LISN que está en contacto con el ESE.

IV. SOLUCIONES PROPUESTAS

A. Interpolación

El método de interpolación corrige la medida de parámetros S en aquellas frecuencias donde el nivel de interferencia generado por el ESE supera el umbral de riesgo para la integridad de la medida. Para determinar si una frecuencia se encuentra por encima de dicho umbral, se han de realizar dos medidas:

- Nivel de interferencia generada por el ESE [dBμV] en sus terminales de línea y neutro a las frecuencias de operación a las cuales se medirán los parámetros S. En este caso el analizador de redes no ha de suministrar potencia alguna ($a_L = a_N = 0$).
- Nivel de las ondas b_L y b_N [dBμV] en los puertos de medida de la configuración empleada (Fig. 3), donde se mezcla la interferencia que genera el ESE con la onda reflejada por éste debido a su impedancia de entrada. En este caso el analizador de redes sí suministra potencia (a_L , $a_N \neq 0$) .

Si la segunda de las medidas no está 12 dB (valor determinado experimentalmente) o más por encima de la primera, se puede considerar que la interferencia del ESE afecta a la medida, por tanto, se deberá corregir la medida de parámetros S a esa frecuencia. Para corregir los parámetros S a una frecuencia de operación, basta con hallar las dos frecuencias más cercanas sin interferencias y realizar una interpolación lineal de sus parámetros S correspondientes. El apartado V de este artículo (validación experimental) muestra medidas sobre equipos reales que validan el correcto funcionamiento de este método.

B. Deembedding

El método *deembedding* compensa, mediante cálculo matemático, el efecto que provoca la LISN, los limitadores de transitorios y los cables de interconexión en la medida de parámetros S del ESE, habiendo tomado como puertos de calibración los puertos del analizador de redes, y no los terminales de la LISN que están en contacto con el equipo

electrónico. La Fig. 4 agrupa los elementos anteriores y los representa como redes de dos y cuatro puertos:

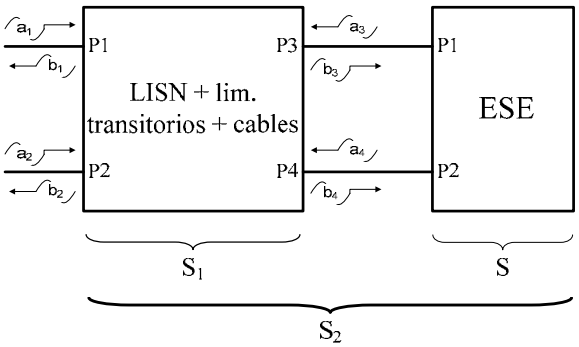

Fig. 4. Definición de puertos del sistema de medida.

Para hallar los parámetros S del ESE (S) será necesario disponer de las siguientes medidas previas:

- Parámetros S del conjunto LISN + limitadores de transitorios + cables (S_1).
- Parámetros S del conjunto LISN + limitadores de transitorios + cables + ESE (S_2).

La matriz de parámetros S relaciona las ondas salientes *b* con las ondas entrantes *a* de cada puerto del ESE [4]:

$$\begin{bmatrix} a_3 \\ a_4 \end{bmatrix} = [S] \cdot \begin{bmatrix} b_3 \\ b_4 \end{bmatrix} \tag{2}$$

Para encontrar la matriz de parámetros S del ESE es necesario expresar a_3 y a_4 en función de b_3 y b_4, lo cual se conseguirá con la ayuda de las matrices S_1 y S_2:

$$\begin{bmatrix} b_1 \\ b_2 \\ b_3 \\ b_4 \end{bmatrix} = [S_1] \cdot \begin{bmatrix} a_1 \\ a_2 \\ a_3 \\ a_4 \end{bmatrix} \tag{3}$$

$$\begin{bmatrix} b_1 \\ b_2 \end{bmatrix} = [S_2] \cdot \begin{bmatrix} a_1 \\ a_2 \end{bmatrix} \tag{4}$$

En [7][8] se presenta el método de cálculo para la extracción de los coeficientes que forman la matriz de parámetros S del ESE a partir de las matrices conocidas S_1 y S_2:

$$\begin{aligned} S_{11} &= \frac{DE - CF}{AD - BC} \;;\; S_{12} = \frac{AF - BE}{AD - BC} \\ S_{21} &= \frac{DG - CH}{AD - BC} \;;\; S_{22} = \frac{AH - BG}{AD - BC} \end{aligned} \tag{5}$$

donde:

$$\begin{aligned} A &= R_{121}S_{211} + R_{122} + R_{123}S_{221} \\ B &= R_{121}S_{212} + R_{124} + R_{123}S_{222} \\ C &= R_{141}S_{211} + R_{142} + R_{143}S_{221} \\ D &= R_{141}S_{212} + R_{144} + R_{143}S_{222} \\ E &= R_{111}S_{211} + R_{112} + R_{113}S_{221} \\ F &= R_{111}S_{212} + R_{114} + R_{113}S_{222} \\ G &= R_{131}S_{211} + R_{132} + R_{133}S_{221} \\ H &= R_{131}S_{212} + R_{134} + R_{133}S_{222} \end{aligned} \tag{6}$$

$$\begin{aligned} R_{111} &= \frac{S_{124}}{S_{124}S_{113} - S_{114}S_{123}} \;;\; R_{121} = \frac{S_{133}S_{124} - S_{134}S_{123}}{S_{124}S_{113} - S_{114}S_{123}} \\ R_{131} &= \frac{S_{123}}{S_{114}S_{123} - S_{113}S_{124}} \;;\; R_{141} = \frac{S_{144}S_{123} - S_{143}S_{124}}{S_{114}S_{123} - S_{113}S_{124}} \\ R_{112} &= \frac{S_{111}S_{124} - S_{121}S_{114}}{S_{123}S_{114} - S_{113}S_{124}} \;;\; R_{132} = \frac{S_{111}S_{123} - S_{113}S_{121}}{S_{113}S_{124} - S_{114}S_{123}} \\ R_{122} &= \frac{S_{131}S_{124} - S_{121}S_{134} + R_{112}\left(S_{133}S_{124} - S_{123}S_{134}\right)}{S_{124}} \\ R_{142} &= \frac{S_{141}S_{123} - S_{143}S_{121} + R_{132}\left(S_{144}S_{123} - S_{143}S_{124}\right)}{S_{123}} \\ R_{113} &= \frac{S_{114}}{S_{123}S_{114} - S_{124}S_{113}} \;;\; R_{123} = \frac{S_{133}S_{114} - S_{134}S_{113}}{S_{123}S_{114} - S_{124}S_{113}} \\ R_{133} &= \frac{S_{113}}{S_{124}S_{113} - S_{123}S_{114}} \;;\; R_{143} = \frac{S_{144}S_{113} - S_{143}S_{114}}{S_{124}S_{113} - S_{123}S_{114}} \\ R_{114} &= \frac{S_{112}S_{124} - S_{122}S_{114}}{S_{123}S_{114} - S_{113}S_{124}} \;;\; R_{134} = \frac{S_{112}S_{123} - S_{113}S_{122}}{S_{113}S_{124} - S_{114}S_{123}} \\ R_{124} &= \frac{S_{132}S_{124} - S_{122}S_{134} + R_{114}\left(S_{133}S_{124} - S_{123}S_{134}\right)}{S_{124}} \\ R_{144} &= \frac{S_{142}S_{123} - S_{143}S_{122} + R_{134}\left(S_{144}S_{123} - S_{143}S_{124}\right)}{S_{123}} \end{aligned} \tag{7}$$

Cuanto más aislados estén los puertos de la LISN entre sí (S_{114}, S_{141}, S_{123}, S_{132}, S_{112}, S_{121}, S_{134}, S_{143} tendiendo a ser nulos), más exactos serán los resultados ofrecidos por la técnica *deembedding*.

V. VALIDACIÓN EXPERIMENTAL

Para validar ambos métodos de medida propuestos (interpolación y *deembedding*) se han realizado medidas a un equipo real: una fuente de alimentación conmutada de 200 W.

A. Interpolación

La Fig. 5 muestra la medida del parámetro S_{11} empleando el método de medida descrito en [4][5], y el método de interpolación presentado en este artículo. Los picos que se observan en métodos anteriores indican una medida de parámetros S incorrecta, debido a que a dichas frecuencias la

interferencia generada por el ESE es del mismo orden de magnitud que la onda reflejada por éste debido a su impedancia de entrada. El método de interpolación corrige este error de medida eliminando dichos picos.

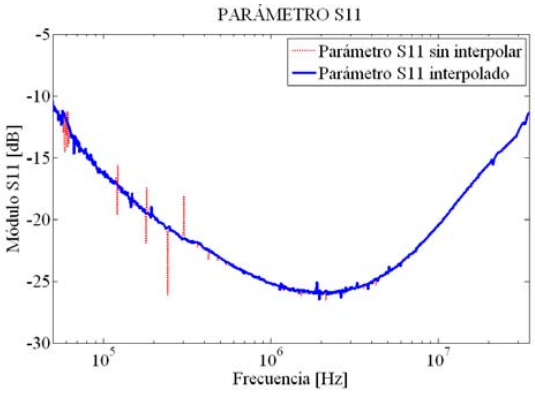

Fig. 5. Comparación parámetro S_{11} con y sin interpolación.

B. Deembedding

La Fig. 6 muestra la medida del parámetro S_{12} empleando el método de calibración en los terminales de la LISN descrito en [4][5], y el método de calibración en los puertos del analizador de redes y posterior aplicación de la técnica *deembedding* presentada en este artículo. Se puede observar como ambos métodos dan resultados muy similares, corroborando su validez. La técnica *deembedding* permitirá pues la utilización de cualquier analizador de redes sin la limitación de calibración impuesta por métodos anteriores.

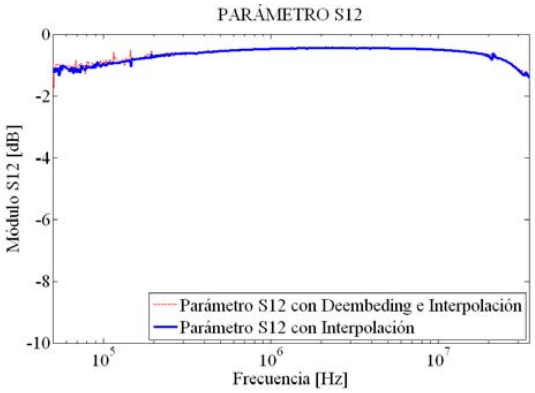

Fig. 6. Comparación parámetro S_{12} con y sin *deembedding*.

VI. CONCLUSIONES

Este artículo presenta y valida dos nuevos métodos que mejoran la medida de parámetros S de equipos electrónicos conectados a la red eléctrica, lo que permitirá una mejor caracterización de la impedancia de entrada del ESE mediante sus modelos equivalentes circuital y modal basados en una red de tres impedancias en pi. Ambos métodos, interpolación y *deembedding*, pueden utilizarse juntos, o de manera independiente, para conseguir dicho propósito.

Los métodos han sido probados utilizando equipos reales, donde se ha demostrado que mejoran los resultados obtenidos respecto a los anteriores métodos de medida.

AGRADECIMIENTOS

Este trabajo ha sido financiado por los proyectos TEC2004-02196 y TEC2005-04238 concedidos por el Ministerio de Educación y Ciencia.

REFERENCIAS

[1] ANSI C63.13, *American National Standard Guide on the Application and Evaluation of EMI Power-Line Filters for Commercial Use*, American National Standards Institute, June 28, 1991

[2] CISPR 17, *Methods of measurement of the suppression characteristics of passive radio interference filters and suppression components*, International Electrotechnical Commission, 1981

[3] J.R. Regué, M. Ribó, D. Duran, D. Badia and A. Pérez, *Common and Differential Mode Characterization of EMI Power-Line Filters from S-parameters Measurements*, Proc. of IEEE International Symposium on EMC, August 9-13, 2004, Santa Clara, CA, pp. 610-615 vol.2

[4] J.R. Regué, M. Ribó, D. Duran, D. Badia and A. Pérez, *Measurement and modeling of noise source impedance of electronic equipment*, Proc. of the 6th EMC Europe International Symposium, September 6-10, 2004, Eindhoven, The Netherlands, pp. 150-154

[5] A. Pérez, J.R. Regué, M. Ribó, A.M. Sánchez, F.J. Pajares, D. Badia, *Circuital Characterization of an Electronic Equipment for Narrow-Band Conducted Emissions*, Proc. of the 7th EMC Europe International Symposium, September 5-8, 2006, Barcelona, Spain, pp. 1035-1040

[6] D.M. Pozar, *Microwave Engineering*, John Wiley & Sons, Inc., USA, 1998

[7] R. Bauer and P. Penfield, *De-embedding and Unterminating*, IEEE Transactions on MTT, March, 1974, vol. MTT-22, pp. 282-288.

[8] *Scorpion Embedding/De-embedding Application Note /GIP*, 11410-00278, May, 2002, http://www.us.anritsu.com/downloads/files/11410-00278B.pdf

Caracterización Circuital de un Equipo Electrónico para Emisiones Conducidas de Banda Estrecha

Antonio Pérez, Joan Ramon Regué, Miquel Ribó, Albert Miquel Sánchez, Javier Pajares, David Badia
antonip@salleurl.edu, jramon@salleurl.edu, mrp@salleurl.edu, albertm@salleurl.edu, fpajares@salleurl.edu, david@salleurl.edu
Departamento de Comunicaciones y Teoría de la Señal
Enginyeria i Arquitectura La Salle, Universitat Ramon Llull
Passeig Bonanova 8, 08022 Barcelona

***Abstract*- In this paper, a new network analyzer-based procedure is presented in order to find the equivalent circuit for conducted interference generation of an electronic equipment when it is connected to the power line. The equivalent circuit is composed by three impedances and two voltage sources, which model the conducted interference that the electronic device supplies to the power line. An accurate model of the interference generation process is very necessary in order to design or choose a suitable power line filter, or to predict the levels of conducted EMI as a function of the impedance presented by the power line. The new procedure is experimentally tested using real measurements.**

I. INTRODUCCIÓN

A la hora de diseñar o seleccionar un filtro de red eficiente es necesaria una completa caracterización del comportamiento del equipo electrónico al cual será conectado, en cuanto a generación de interferencia se refiere, para poder predecir la atenuación real del filtro, y los niveles de interferencia que el dispositivo filtrado suministrará a la red eléctrica en forma de emisión conducida.

En [1], se presenta una caracterización completa de un filtro de red. Éste es caracterizado mediante sus parámetros S, físicos y modales. Esta caracterización es más general que aquellas basadas sólo en la computación separada de las atenuaciones en modo común y diferencial [2], ya que tiene en cuenta interferencias espurias que fluyen entre puertos debido a asimetrías en el diseño de los filtros, de modo común a diferencial y viceversa. Para que esta caracterización sea útil en un contexto de diseño, una caracterización similar, que considere los puertos físicos del equipo electrónico (línea-tierra y neutro-tierra) o sus equivalentes modales (común y diferencial), ha de ser empleada.

En [3], se presenta un modelo completo (usando puertos físicos y modales) para la impedancia del equipo electrónico (vista desde los cables de alimentación). El dispositivo electrónico se modela mediante un circuito equivalente de tres impedancias en pi, el cual se obtiene a partir de la medida de parámetros S, considerando el equipo como un dispositivo de dos puertos: línea-tierra y neutro-tierra. A partir de este modelo, se obtiene un nuevo modelo modal equivalente, mediante el cual se puede predecir la atenuación actual de un filtro de red conectado al equipo electrónico. Pero, debido a la falta de información acerca de las fuentes de interferencia, este modelo no puede ser utilizado para predecir el nivel de interferencia generado por el dispositivo electrónico después del filtro de red.

En este artículo se presenta y valida un modelo circuital completo para la generación de interferencia conducida de un ESE (Equipo Sometido a Ensayo). Éste extiende los resultados de [3] (proporcionando algunas modificaciones que serán descritas a continuación), y propone una nueva técnica de medida, también basada en analizador de redes y LISN, con objeto de obtener un circuito equivalente más completo, compuesto por una red de tres impedancias en pi y dos fuentes de tensión, que modelan la interferencia de banda estrecha generada por el equipo electrónico. El procedimiento es válido para frecuencias dentro de la banda de trabajo de la LISN. Puesto que este modelo contiene fuentes de tensión que modelan las fuentes de interferencia con precisión, puede ser utilizado para predecir los niveles de interferencia cuando el ESE está conectado a cualquier carga (filtro de red, red eléctrica, etc.).

II. MODELO CIRCUITAL EQUIVALENTE

Desde el punto de vista de una EMI conducida, los tres terminales de alimentación de un ESE (Fig. 1) se pueden analizar como una red de dos puertos (Fig. 2). El puerto "L" se define entre el terminal de línea y el terminal de tierra, y el puerto "N" se define entre los terminales de neutro y tierra.

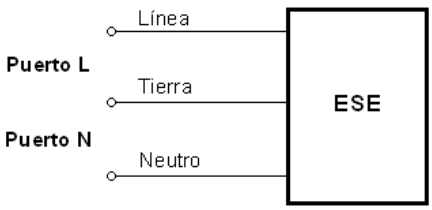

Fig. 1. Definición de puertos para el ESE.

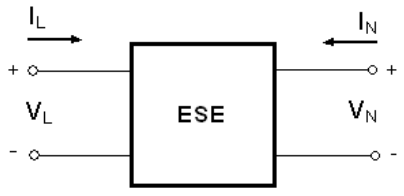

Fig. 2. Circuito equivalente de dos puertos para el ESE.

El ESE de la Fig. 2 se puede modelar mediante una red de tres impedancias en pi más dos fuentes externas de interferencia conectadas en serie a los terminales "L" y "N" (Fig. 3) [4]. Estas fuentes equivalentes generan la misma interferencia en los terminales que las fuentes interferentes internas del ESE.

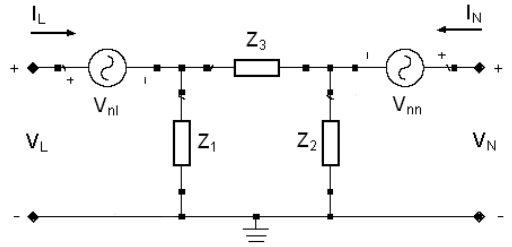

Fig. 3. Modelo circuital para el ESE.

A. Red de tres impedancias en pi

Las tres impedancias (Z1, Z2 y Z3) del modelo circuital de la Fig. 3 se pueden hallar a partir de la medida de parámetros S en ambos puertos del ESE:

$$Z_1 = \frac{Z_0\left(1+S_{11}\right)\left(1+S_{22}\right)-Z_0S_{12}S_{21}}{\left(1-S_{11}\right)\left(1+S_{22}\right)+S_{12}S_{21}-2S_{21}}$$
$$Z_2 = \frac{Z_0\left(1+S_{11}\right)\left(1+S_{22}\right)-Z_0S_{12}S_{21}}{\left(1+S_{11}\right)\left(1-S_{22}\right)+S_{12}S_{21}-2S_{21}} \quad (1)$$
$$Z_3 = \frac{Z_0\left(1+S_{11}\right)\left(1+S_{22}\right)-Z_0S_{12}S_{21}}{2S_{21}}$$

donde Z_0 es la impedancia de referencia del sistema de medida, el puerto 1 es el puerto "L" y el puerto 2 es el puerto "N".

En [3], los parámetros S medidos se convierten en parámetros ABCD, y de estos se extraen los valores de las tres impedancias. En este artículo las impedancias se encuentran directamente a partir de los parámetros S medidos, obteniendo un sistema mejor condicionado que reduce la propagación de errores.

B. Fuentes de interferencia

Los valores de las dos fuentes de tensión externas de interferencia (V_{nl}, V_{nn}) presentes en el modelo circuital de la Fig. 3, se hallan a partir de la medida (sistema de medida descrito a continuación) de tensiones y corrientes en los terminales del ESE: V_L, I_L, V_N e I_N. La relación entre estos parámetros es:

$$I_L = \frac{V_L - V_{nl}}{Z_1} + \frac{V_L - V_{nl} - V_N + V_{nn}}{Z_3}$$
$$I_N = \frac{V_N - V_{nn}}{Z_2} + \frac{V_N - V_{nn} - V_L + V_{nl}}{Z_3} \quad (2)$$

De estas ecuaciones se pueden aislar las dos fuentes externas de tensión interferentes (V_{nl}, V_{nn}):

$$V_{nl} = V_L - \frac{Z_1\left(Z_2+Z_3\right)I_L + Z_1Z_2I_N}{Z_1+Z_2+Z_3}$$
$$V_{nn} = V_N - \frac{Z_2\left(Z_1+Z_3\right)I_N + Z_1Z_2I_L}{Z_1+Z_2+Z_3} \quad (3)$$

III. SISTEMA DE MEDIDA

La configuración utilizada para medir las tensiones e intensidades en los terminales del ESE (Fig. 4) consiste de un analizador de redes y una red de acoplamiento (LISN). La red de acoplamiento acopla los puertos de RF del analizador de redes a los puertos "L" y "N" del ESE, y protege al analizador de la elevada tensión de la red eléctrica (50 Hz), por lo que ha sido adoptada para la medida que ocupa.

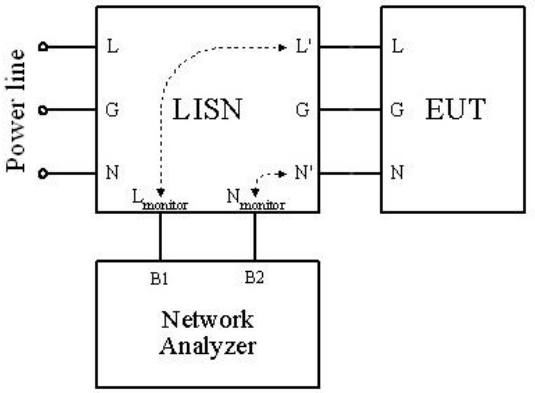

Fig. 4. Diagrama de bloques del sistema de medida.

Los conectores de alimentación de la LISN se conectan al ESE al igual que en un ensayo de emisión conducida, mientras que los conectores de monitorización de la línea y el neutro se llevan a ambos puertos del analizador. El analizador de redes ha de disponer de dos entradas de impedancia Z_0 para medir el módulo de las tensiones presentes en ambos puertos del ESE y la fase relativa entre ellas. El conjunto formado por ESE, analizador de redes, LISN y cableado se puede representar como en Fig. 5.

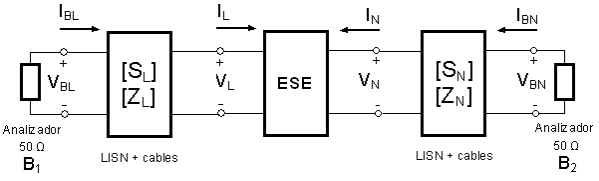

Fig. 5. Circuito equivalente del sistema de medida.

El analizador de redes mide los valores de las tensiones V_{BL} (amplitud y fase de referencia (nula)) y V_{BN} (amplitud y fase relativa a V_{BL}). Por tanto, es necesario compensar los efectos de la LISN y los cables para obtener las tensiones V_L y V_N, ya que éstas son las que permiten computar las fuentes de tensión interferentes V_{nl} y V_{nn} (ecuación (3)), y no las tensiones medidas V_{BL} y V_{BN}. Para hallar el valor de V_L y V_N:

1. Medir los parámetros S del conjunto formado por LISN y cables de interconexión (S_L y S_N).

2. Transformar los parámetros S_L y S_N en parámetros Z_L y Z_N mediante las siguientes expresiones [5]:

$$
\begin{aligned}
Z_{11} &= \frac{Z_0\left(1+S_{11}\right)\left(1-S_{22}\right)+Z_0S_{12}S_{21}}{\left(1-S_{11}\right)\left(1-S_{22}\right)-S_{12}S_{21}} \\
Z_{12} &= \frac{2Z_0S_{12}}{\left(1-S_{11}\right)\left(1-S_{22}\right)-S_{12}S_{21}} \\
Z_{21} &= \frac{2Z_0S_{21}}{\left(1-S_{11}\right)\left(1-S_{22}\right)-S_{12}S_{21}} \\
Z_{22} &= \frac{Z_0\left(1-S_{11}\right)\left(1+S_{22}\right)+Z_0S_{12}S_{21}}{\left(1-S_{11}\right)\left(1-S_{22}\right)-S_{12}S_{21}}
\end{aligned}
\tag{4}
$$

3. Medir las tensiones V_{BL} y V_{BN} (ambas amplitudes y fase relativa).
4. Hallar las tensiones V_L y V_N, y las corrientes I_L e I_N, utilizando las siguientes expresiones:

$$
\begin{aligned}
V_L &= Z_{21L}I_{BL}-Z_{22L}I_L \\
V_N &= Z_{21N}I_{BN}-Z_{22N}I_N \\
I_L &= \frac{Z_{11L}I_{BL}-V_{BL}}{Z_{12L}} \\
I_N &= \frac{Z_{11N}I_{BN}-V_{BN}}{Z_{12N}}
\end{aligned}
\tag{5}
$$

$$
\begin{aligned}
I_{BL} &= -\frac{V_{BL}}{Z_0} \\
I_{BN} &= -\frac{V_{BN}}{Z_0}
\end{aligned}
\tag{6}
$$

donde Z_0 es la impedancia de referencia del sistema de medida (50 Ω en nuestro caso). Substituyendo la ecuación (6) en (5) se obtiene las tensiones y corrientes en los terminales del ESE:

$$
\begin{aligned}
V_L &= V_{BL}\left(\frac{Z_{22L}}{Z_{12L}}+\frac{Z_{11L}Z_{22L}}{Z_0Z_{12L}}-\frac{Z_{21L}}{Z_0}\right) \\
V_N &= V_{BN}\left(\frac{Z_{22N}}{Z_{12N}}+\frac{Z_{11N}Z_{22N}}{Z_0Z_{12N}}-\frac{Z_{21N}}{Z_0}\right) \\
I_L &= -V_{BL}\left(\frac{Z_{11L}}{Z_0Z_{12L}}+\frac{1}{Z_{12L}}\right) \\
I_N &= -V_{BN}\left(\frac{Z_{11N}}{Z_0Z_{12N}}+\frac{1}{Z_{12N}}\right)
\end{aligned}
\tag{7}
$$

5. Finalmente, se calculan las fuentes equivalentes de interferencia V_{nl} y V_{nn} utilizando la ecuación (3).

IV. Validación experimental y resultados

A. Validación experimental

Para validar el modelo propuesto y el método de medida, se ha implementado y medido un circuito de prueba (ESE) como el representado en Fig. 6.

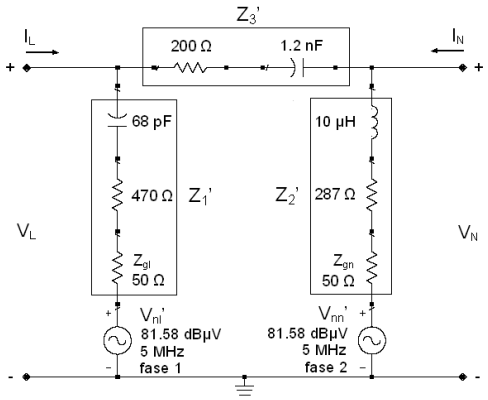

Fig. 6. Circuito de prueba para validación experimental.

Se ha implementado el circuito de Fig. 6, y no uno con la estructura de Fig. 3, porque en Fig. 6 los dos generadores tienen referencia común, por lo que es más fácil implementarlos utilizando instrumentación de laboratorio. Las fuentes interferentes V_{nl}' y V_{nn}' se han implementado usando un generador de RF y un divisor de potencia con dos salidas de igual amplitud y diferencia de fase 180º.

Los valores teóricos del modelo circuital (Fig. 3) para el circuito de prueba de Fig. 6 se obtienen mediante las siguientes expresiones:

$$
\begin{aligned}
Z_1 &= Z_1' \\
Z_2 &= Z_2' \\
Z_3 &= Z_3' \\
V_{nl} &= \frac{\left(Z_2+Z_3\right)V_{nl}'+Z_1V_{nn}'}{Z_1+Z_2+Z_3} \\
V_{nn} &= \frac{\left(Z_1+Z_3\right)V_{nn}'+Z_2V_{nl}'}{Z_1+Z_2+Z_3}
\end{aligned}
\tag{8}
$$

La tabla I muestra los valores de las tres impedancias (Z_1', Z_2' y Z_3') del circuito de prueba de Fig. 6, las cuales coinciden con las tres impedancias (Z_1, Z_2 y Z_3) del modelo circuital de Fig. 3, obtenidas de dos maneras distintas:

- Columna 1: valores medidos de las impedancias (medidas una a una con el analizador de redes).
- Columna 2: valores calculados de las impedancias a partir de los parámetros S medidos (sección II.A) usando la configuración de medida descrita en [3].

Tabla I. Medida impedancias red en pi.

	Z medida individual [Ω]	*Z calculada param-S [Ω]*
Z_1	525 - j474	489 - j486
Z_2	335 + j310	350 + j314
Z_3	203 - j24	201 - j26

La Tabla II lista las amplitudes y las fases de las fuentes interferentes del modelo circuital (Fig. 3) para el circuito de prueba de Fig. 6: valores teóricos (usando ecuación (8)) y valores medidos (usando el procedimiento descrito en la sección III y empleando la configuración de medida de Fig. 4). Como se puede observar, las amplitudes de las fuentes interferentes deducidas a partir de las medidas realizadas coinciden con las teóricas (dentro de 1 dB de error), como también la diferencia de fase, la cual es de 26.91º para el valor teórico, y de 27.95º para el valor medido. Por tanto, queda demostrado que existe una coincidencia entre los valores teóricos del circuito y los calculados a partir de las medidas realizadas. Este hecho valida el método de medida propuesto anteriormente para la obtención de un modelo circuital equivalente del ESE.

Tabla II. Medida fuentes interferentes.

	Fuentes teóricas nivel [dBμV]; fase [º]	*Fuentes medidas nivel [dBμV] ; fase [º]*
V_{nl}	78.53 ; 0	77.43 ; 0
V_{nn}	79.98 ; 26.91	79.05 ; 27.95

B. Modelo circuital de una fuente de alimentación conmutada

Este apartado tiene como objeto hallar el modelo circuital equivalente de un ESE real, como es el caso de una fuente de alimentación conmutada de ordenador personal de 200 W. Se principia por realizar una medida de emisión conducida del equipo, según CISPR 22, en ambos puertos del equipo (puertos "L" y "N"). De esta manera se identifican las principales frecuencias interferentes del dispositivo dentro del margen de medida (150 kHz a 30 MHz) (Fig. 7). Se comprueba que la emisión conducida en ambos puertos es muy similar, y que las interferencias son de banda estrecha.

A continuación, y para cada una de las frecuencias en las que se ha detectado un nivel de interferencia superior o cercano al límite establecido por la norma, se halla el modelo circuital equivalente (Fig. 3). A modo de ejemplo, la Tabla III lista los parámetros del modelo de la Fig. 3 para una interferencia de 602,17 kHz.

Tabla III. Parámetros del modelo circuital a 602,17 KHz.

Z_1	486 – j2014 Ω
Z_2	2654 – j1679 Ω
Z_3	6.2 – j1.4 Ω
V_{nl}	59.82 dBμV ; 183 º
V_{nn}	65.01 dBμV ; 166 º

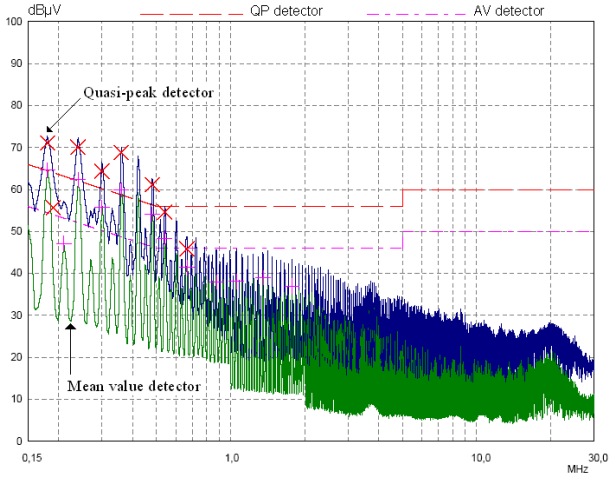

Fig. 7. Medida de la emisión conducida en el puerto "L".

V. CONCLUSIONES

Este artículo presenta y valida un método de medida útil para hallar un modelo circuital equivalente, lo más general posible, que caracterice el comportamiento de un ESE en cuanto a emisión conducida de banda estrecha se refiere. El procedimiento de medida dispone de una configuración similar a la utilizada en un ensayo de emisión conducida, pero utilizando un analizador de redes en vez de un receptor de EMI.

El modelo circuital presentado se puede utilizar también para caracterizar el comportamiento de la red eléctrica en cuanto a impedancia e interferencia concierne. Para conseguir esto, sólo unos pequeños cambios en el método de medida descrito serían suficientes.

El nuevo modelo y procedimiento de medida ha sido probado utilizando un circuito de prueba conocido, prediciendo con precisión sus parámetros. Finalmente, se ha aplicado el proceso de caracterización a una fuente de alimentación conmutada.

AGRADECIMIENTOS

Este trabajo ha sido financiado por los proyectos TEC2004-02196 y TEC2005-04238 concedidos por el Ministerio de Educación y Ciencia.

REFERENCIAS

[1] J.R. Regué, M. Ribó, D. Duran, D. Badia and A. Pérez, *Common and Differential Mode Characterization of EMI Power-Line Filters from S-parameters Measurements*, Proc. of IEEE International Symposium on EMC, August 9-13, 2004, Santa Clara, CA, pp. 610-615 vol.2

[2] ANSI C63.13, *American National Standard Guide on the Application and Evaluation of EMI Power-Line Filters for Commercial Use*, American National Standards Institute, June 28, 1991

[3] J.R. Regué, M. Ribó, D. Duran, D. Badia and A. Pérez, *Measurement and modeling of noise source impedance of electronic equipment*, Proc. of the 6th EMC Europe International Symposium, September 6-10, 2004, Eindhoven, The Netherlands, pp. 150-154

[4] Guillermo González, *Microwave Transistor Amplifiers (2nd edition)*, Prentice-Hall, Inc., USA, 1997.

[5] D.M. Pozar, *Microwave Engineering*, John Wiley & Sons, Inc., USA, 1998.

Caracterización modal de filtros de red a partir de parámetros S

Dani Durán, Joan Ramón Regué, Miquel Ribó, David Badia, Antonio Pérez
Departamento de Comunicaciones y Teoría de la Señal
Enginyeria i Arquitectura La Salle, Universitat Ramon Llull
Passeig Bonanova 8, 08022 Barcelona
danid@salleurl.edu, jramon@salleurl.edu, mrp@salleurl.edu, david@salleurl.edu, antonip@salleurl.edu

***Abstract*- The current method of measuring the behaviour of power line filters, based only in common and differential mode attenuations, is not capable to predict the efficiency of the filter in any environment. If the filter is between line and load impedances different from 50 Ω, its efficiency may be decreased and the filter may not work as expected. Besides, signals injected to the filter in a certain mode, can be converted to the other mode at the output, being undetected by the current measurement method. In this paper a new method to characterize power line filters, based on S parameters measurements, is presented. It is capable to determine the energy transfer between any combination of input and output modes, and to predict the behaviour of the filter with any source and load impedances.**

I. INTRODUCCIÓN

Los filtros de red son ampliamente usados para atenuar las emisiones conducidas de cualquier dispositivo que deba conectarse a la red de alimentación. Para cumplir con la normativa de compatibilidad electromagnética (EMC), las emisiones no deben sobrepasar un cierto nivel.

Los métodos normalmente usados para caracterizar los filtros de red [1], [2] están basados en medidas de atenuación en modo común y modo diferencial con impedancias de carga y de generador de 50 Ω.

Estos métodos no resultan útiles para predecir el comportamiento del filtro en un entorno real, en el cual las impedancias que se presentan pueden ser muy diferentes de 50 Ω.

Los parámetros S caracterizan completamente el comportamiento de un circuito de RF, y por lo tanto pueden usarse para caracterizar un filtro de red [3].

En este artículo presentamos un nuevo método para caracterizar el comportamiento en modo común y diferencial de un filtro de red basado en medidas de parámetros S, el cual es capaz de predecir la transferencia de energía entre cualquier combinación de modos de entrada y salida, así como el comportamiento del filtro con cualquier impedancia de generador y de carga.

II. PROCEDIMIENTO

Supongamos que disponemos de los parámetros S de un filtro de red bipolar típico, como se muestra en la figura 1(a). Dicho filtro tiene cuatro puertos, cada uno de ellos es referenciado al terminal de tierra del mismo. La matriz de parámetros S medida, relaciona las ondas salientes b con las ondas entrantes a de cada puerto del filtro.

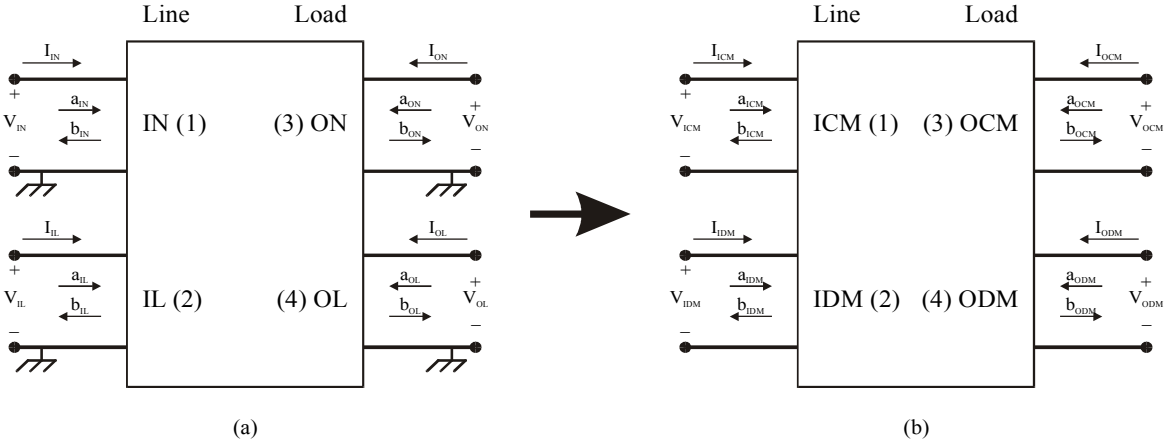

Fig. 1: Definición de puertos de los parámetros S: medidos (a) y modales (b).

$$[b]=\begin{bmatrix} b_{IN} \\ b_{IL} \\ b_{ON} \\ b_{OL} \end{bmatrix} \quad [a]=\begin{bmatrix} a_{IN} \\ a_{IL} \\ a_{ON} \\ a_{OL} \end{bmatrix} \tag{2}$$

Como nuestro interés reside en el comportamiento en modo común y diferencial del filtro de red, necesitamos obtener una
nueva matriz de parámetros S que relacione los modos común y diferencial de entrada con los modos común y diferencial de salida (figura 1(b)). Esta nueva matriz llamada S_M (parámetros S modales) relaciona las ondas salientes b_M con las ondas entrantes a_M de cada modo.

$$[b_M]=[S_M]\cdot[a_M] \tag{3}$$

$$[b_M]=\begin{bmatrix} b_{ICM} \\ b_{IDM} \\ b_{OCM} \\ b_{ODM} \end{bmatrix} \quad [a_M]=\begin{bmatrix} a_{ICM} \\ a_{IDM} \\ a_{OCM} \\ a_{ODM} \end{bmatrix} \tag{4}$$

El objetivo de este cálculo es obtener la matriz modal S_M a partir de la matriz medida S.

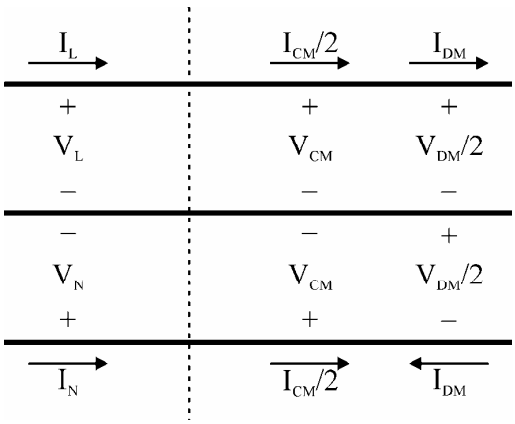

Fig. 2: Definición de las tensiones y corrientes modales en las líneas de alimentación.

La relación de las ondas a y b con las tensiones y corrientes en cada puerto es la siguiente :

$$\begin{aligned} a_L &= \frac{1}{2\sqrt{Z_0}}\left(V_L + Z_0 I_L\right) \\ a_N &= \frac{1}{2\sqrt{Z_0}}\left(V_N + Z_0 I_N\right) \\ b_L &= \frac{1}{2\sqrt{Z_0}}\left(V_L - Z_0 I_L\right) \\ b_N &= \frac{1}{2\sqrt{Z_0}}\left(V_N - Z_0 I_N\right) \\ a_{CM} &= \frac{1}{2\sqrt{Z_{0CM}}}\left(V_{CM} + Z_{0CM} I_{CM}\right) \\ a_{DM} &= \frac{1}{2\sqrt{Z_{0DM}}}\left(V_{DM} + Z_{0DM} I_{DM}\right) \\ b_{CM} &= \frac{1}{2\sqrt{Z_{0CM}}}\left(V_{CM} - Z_{0CM} I_{CM}\right) \\ b_{DM} &= \frac{1}{2\sqrt{Z_{0DM}}}\left(V_{DM} - Z_{0DM} I_{DM}\right) \end{aligned} \tag{5}$$

Analizando las relaciones entre las tensiones y corrientes de la figura 2, obtenemos el siguiente resultado :

$$\begin{aligned} V_{CM} &= \frac{V_L + V_N}{2} \qquad I_{CM} = I_L + I_N \\ V_{DM} &= V_L - V_N \qquad I_{DM} = \frac{I_L - I_N}{2} \end{aligned} \tag{6}$$

Sustituyendo (6) en (5) podemos escribir las siguientes ecuaciones relacionando ondas medidas con ondas modales :

$$\begin{aligned} a_{CM} &= \frac{a_L}{\sqrt{2}} + \frac{a_N}{\sqrt{2}} \qquad b_{CM} = \frac{b_L}{\sqrt{2}} + \frac{b_N}{\sqrt{2}} \\ a_{DM} &= \frac{a_N}{\sqrt{2}} - \frac{a_L}{\sqrt{2}} \qquad b_{DM} = \frac{b_N}{\sqrt{2}} - \frac{b_L}{\sqrt{2}} \end{aligned} \tag{7}$$

Donde :

$$\begin{aligned} Z_{0CM} &= \frac{Z_0}{2} \\ Z_{0DM} &= 2Z_0 \end{aligned} \tag{8}$$

En (7), podemos deducir dos relaciones matriciales entre ondas medidas y modales

$$[a_M]=[A]\cdot[a] \tag{9}$$

$$[b_M]=[B]\cdot[b] \tag{10}$$

Donde:

$$[A]=[B]=\frac{1}{\sqrt{2}}\begin{bmatrix}1 & 1 & 0 & 0\\ -1 & 1 & 0 & 0\\ 0 & 0 & 1 & 1\\ 0 & 0 & -1 & 1\end{bmatrix} \quad (11)$$

Sustituyendo (9) y (10) en (1) obtenemos la relación entre los parámetros S modales y los parámetros S medidos.

$$[S_M]=[B]\cdot[S]\cdot[A]^{-1} \quad (12)$$

Usando (12) podemos obtener la matriz de parámetros S modales, con la que se describe completamente el comportamiento modal de un filtro de red, a partir de una matriz de parámetros S que puede medirse de forma muy simple.

III. APLICACIONES

La aplicación principal es determinar la atenuación en modo común y diferencial de un filtro de red, mirando los parámetros S_{M31} y S_{M42} respectivamente. En la figura 3 vemos la comparación entre la atenuación en modo común de un filtro usando los parámetros S modales y midiendo de acuerdo con [1], donde se observa que el error es muy pequeño. De igual forma, puede determinarse la atenuación en modo diferencial y también extraer la información de fase de cualquiera de los modos.

Además, el método permite hallar la transferencia de energía entre cualquier combinación de modos de entrada y salida.

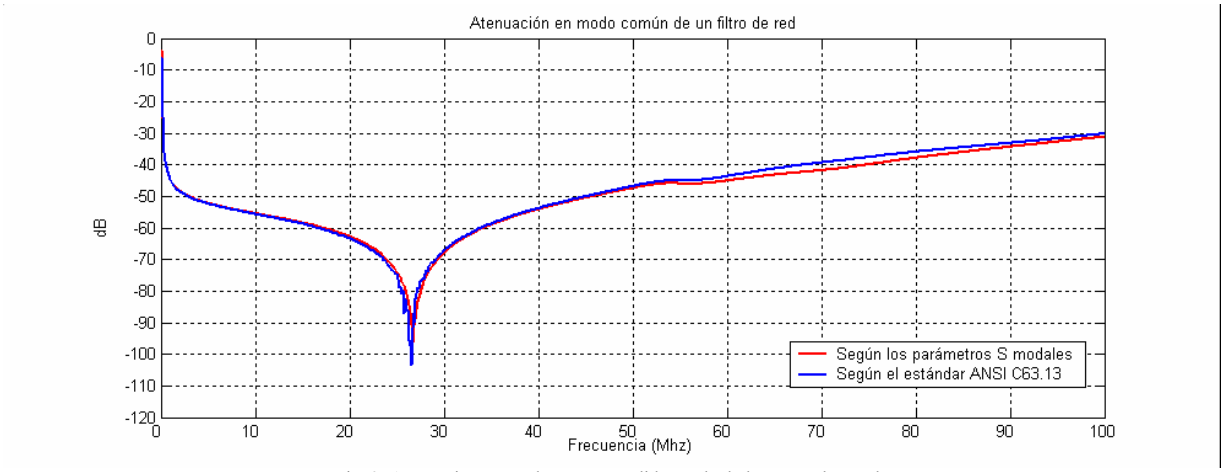

Fig. 3: Atenuación en modo común medida y calculada según el método

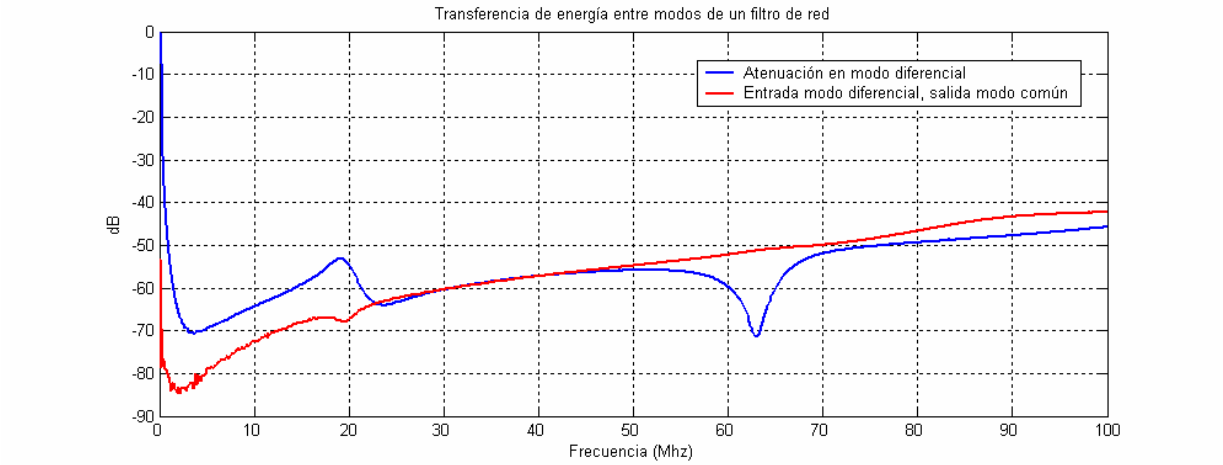

Fig. 4: Transferencia de energía entre la entrada en modo diferencial y los modos de salida común y diferencial

Por ejemplo, la figura 4 muestra la transferencia de energía entre el modo común en la entrada y el modo diferencial en la salida de un filtro previamente medido en parámetros S. Se puede observar como a partir de aproximadamente 23 MHz, si inyectamos una señal en modo diferencial, la mayor parte de la potencia sale en modo común, lo cual no es detectado por el actual método de medida [1].

Por último, como el filtro está totalmente caracterizado por su matriz de parámetros S, es posible simular su eficiencia con cualquier impedancia de generador y de carga. En la figura 5, vemos como cargas diferentes pueden variar notablemente la atenuación en modo común de un filtro de red.

IV. CONCLUSIONES

Se ha presentado una nuevo método de medida para filtros de red basado en parámetros S. Este método, además de predecir los valores de atenuación en modo diferencial y común del mismo modo que podía hacerse mediante la medida definida en [1], permite ver la transferencia de energía entre cualquier combinación de modos de entrada y salida, y también predecir el comportamiento que tendrá el filtro con cualesquiera que sean las impedancias de generador y carga.

REFERENCIAS

[1] ANSI C63.13, "American National Standard Guide on the Application and Evaluation of EMI Power-Line Filters for Commercial Use," American National Standards Institute, June 28, 1991.

[2] CISPR 17, "Methods of measurement of the suppression characteristics of passive radio interference filters and suppression components," International Electrotechnical Commission, 1981.

[3] J. G. Kraemer, "S-parameter Characterization for EMI filters," in Proc. 2003 IEEE EMC Symp., Boston, MA, Aug. 18–22, 2003, pp. 361–366.

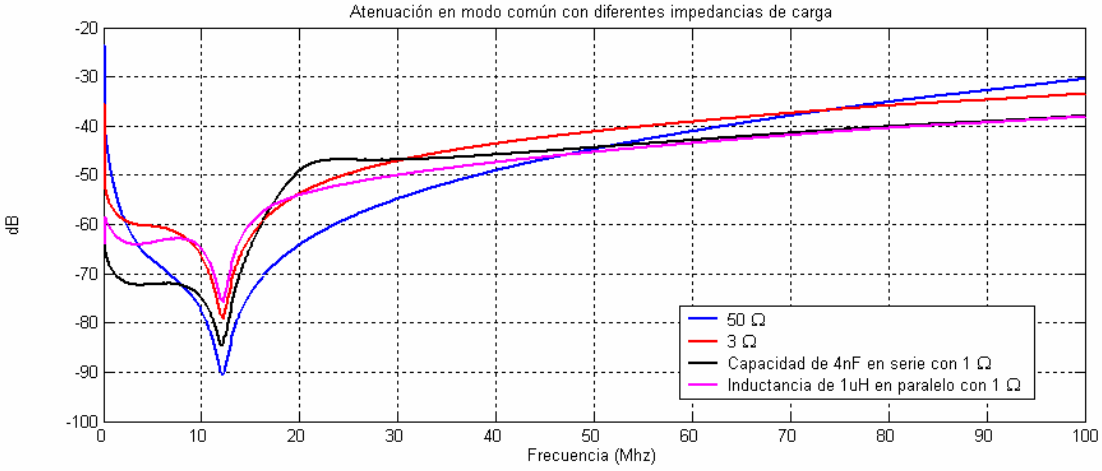

Fig. 5: Atenuación en modo común con diferentes impedancias de carga.

Universitat Ramon Llull

Aquesta Tesi Doctoral ha estat defensada el dia ____ d _____ de ____

al Centre _____

de la Universitat Ramon Llull

davant el Tribunal format pels Doctors sotasignants, havent obtingut la qualificació:

President/a

_____

Vocal

_____

Vocal

_____

Vocal

_____

Secretari/ària

_____

Doctorand/a

C. Claravall, 1-3
08022 Barcelona
Tel. 936 022 200
Fax 936 022 249
E-mail: urlsc@sec.url.es
www.url.es